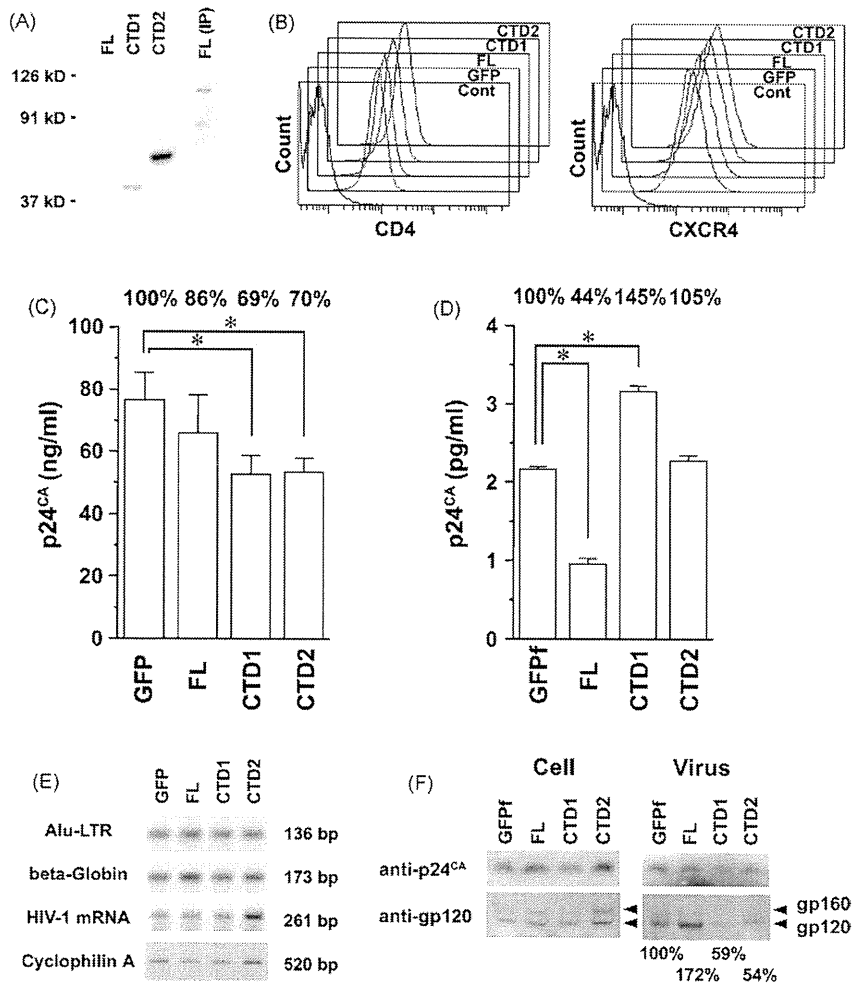

Fig. 2. Functional characterization of the SEC14L1a derivatives. (A) Detection of stable expression of FL, CTD1, and CTD2 in MT-4 cells by Western blotting using anti-FLAG antibody. FL was detected by the immunoprecipitation (IP) assay using agarose beads conjugated with anti-FLAG antibody. The flow cytometric analysis of the cell surface expression of HIV-1 receptors CD4 and CXCR4 in MT-4 cells stably expressing GFP, FL, CTD1, and CTD2. (C) Constitutive expression of CTD1 and CTD2 limited the replication of HIV-1 in MT-4 cells. The concentration of viral $p24^{CA}$ antigen in the culture supernatant was measured at 4 d post-infection. The results represent the average of seven independent experiments ± the standard error of the mean. The reduction of viral $p24^{CA}$ concentration relative to GFP was shown on the top. Asterisks indicate the statistical significance compared to GFP ($P < 0.05$ by two-tailed Student's *t*-test). (D) The PCR-based assay to examine the effect of SEC14L1a derivatives on the early phase of viral life cycle (top two panels) and the transcription from LTR promoter (bottom two panels). The HIV-1 entry efficiency was examined by Alu-LTR PCR. Beta globin was used as an internal control. The HIV-1 transcription efficiency was examined by RT-PCR targeting spliced viral mRNA. Cyclophilin A was used as a control. The expected length of each PCR amplicon was indicated. (E) The effect of SEC14L1a derivatives on the HIV-1 production. The 293T cells grown in a well of a 6-well plate were transfected with 200 ng of HIV-1 proviral DNA and 2 μg of expression vector for GFPf, FL, CTD1, or CTD2. The culture supernatant was recovered at 2 d post-transfection and the $p24^{CA}$ concentration was measured. The representative data from five independent experiments was shown. The results indicate the average ± the standard deviation. The relative $p24^{CA}$ concentration compared to GFPf was shown on the top. Asterisks indicate the statistical significance compared to GFPf ($P < 0.001$ by two-tailed Student's *t*-test). The *Env* incorporation onto the virus-like particles (VLP) produced by 293T cells expressing SEC14L1a derivatives. The 293T cells grown in a well of a 6-well plate were transfected with 1 μg of *gag-pol* (pCMVR8.91) and *Env* (pIIIex) expression vectors along with 2 μg of expression vector for GFPf, FL, CTD1, or CTD2. The cell lysates (Cell) and VLP fractions (Virus) were subjected to Western blot analysis detecting gp120 and $p24^{CA}$ harvested at 2 d post-transfection. The *Env* incorporation levels normalized to $p24^{CA}$ relative to GFPf were shown at the bottom.

G-pseudotyped HIV-1 vector, and the cellular genomic DNA was recovered at 4 d post-infection. The amount of Alu-LTR PCR products from FL-, CTD1-, or CTD2-expressing MT-4 cells was almost equal to that from GFP-expressing cells, suggesting that the early phase of the viral life cycle is not inhibited by any of the SEC14L1a derivatives (Fig. 2D). To examine the viral production phase, we examined the LTR-driven viral gene transcription by RT-PCR. Cellular RNA was extracted from the same MT-4 cells infected with VSV-G-pseudotyped HIV-1 vector, and RT-PCR was conducted to amplify LTR promoter-driven spliced HIV-1 mRNA. The amount of viral RNA expressed in FL-, CTD1-, or CTD2-expressing cells was not lower than that in GFP-expressing cells when the levels of the internal control was taken into account (Fig. 2D). Given that the similar number of viral genome was integrated as indicated by the Alu-LTR PCR, these data suggest that viral transcription is not inhibited by any of the SEC14L1a derivatives, and that the action point of CTD1 and CTD2 should be at post-transcriptional levels of the viral production phase.

Next, the FL, CTD1, or CTD2 expression vector was co-transfected with HIV-1 proviral DNA into 293T cells, and viral production was quantified by $p24^{CA}$ ELISA. The FLAG-tagged GFP (GFPf) was used as a control hereafter. We found that the FL expression significantly reduced the production of HIV-1 (44.2%, $P < 0.001$, two-tailed Student's *t*-test) compared to the GFPf control (Fig. 2E). In contrast, the CTD1 enhanced the production of HIV-1 (145.9%, $P < 0.001$, two-tailed Student's *t*-test; Fig. 2E). However, CTD2 did not measurably affect the HIV-1 production (105.1%, not statistically significant; Fig. 2E). As the ELISA assay examines the effect

Please cite this article in press as: Urano E, et al. T cell-based functional cDNA library screening identified SEC14-like 1a carboxy-terminal domain as a negative regulator of human immunodeficiency virus replication. Vaccine (2009), doi:10.1016/j.vaccine.2009.07.084

of CTDs on *Gag* functions, we next tested the functional interaction between CTDs and *Env*. The *Env* incorporation onto the virion was examined by tripartite-transfection of expression vectors for *Env*, *gag-pol*, and SEC14L1a derivatives into 293T cells, and the VLP was collected by centrifugation. The immunoblotting against gp120 was performed on the cell lysate and the VLP fraction. The cellular *Env* and *Gag* expressions were not detectably affected by any of the SEC14L1a derivatives (Fig. 2F, left panel). The *Env* incorporation onto the VLP was slightly enhanced by FL (157%; Fig. 2F, right panel). In contrast, the VLP produced from CTD1- or CTD2-expressing cells incorporated substantially fewer *Env* than those from GFPf-expressing cells (59% or 54%, respectively; Fig. 2F, right panel). These data were reproducible in independently performed experiments. The densitometric analysis of Western blot image showed that the average ± the standard error of the mean of Env incorporation onto the virion was 129.7 ± 39.9%, 54.8 ± 24.7%, and 25.5 ± 10.3% for FL, CTD1, and CTD2 compared to GFPf, respectively (3–4 independent experiments). The *Env*-mediated cell-to-cell fusion assay indicated that SEC14L1a derivatives did not limit the cell surface targeting and function of *Env* (data not shown). In addition, the *Gag* processing in virion was unaffected by any of the SEC14L1a derivatives (data not shown). Collectively, these data suggest that the HIV-1 replication is inhibited by CTD1 and CTD2 due to the inefficient *Env* incorporation onto the virion. To test this possibility, we infected fresh MT-4 cells with the equal amount of HIV-1 propagated in CTD1- or CTD2-expressing MT-4 cells (1–2 ng $p24^{CA}$), and the viral replication was monitored at 3–4 days post-infection by measuring the $p24^{CA}$ concentration. The infectivity of HIV-1 propagated in CTD1- or CTD2-expressing cells was attenuated to 83.1 ± 17.9% or 82.4 ± 5.5% relative to the virus recovered from GFP-expressing cells, respectively (the average ± the standard error of the mean of 3 independent experiments). Altogether, these data suggest that the inhibition of HIV-1 replication by CTD1 and CTD2 is attributed to the attenuation of viral infectivity by lowering the *Env* incorporation onto the virion.

4. Discussion

In the present study, we provide the first evidence that the C-terminal fragment of SEC14L1a functions as an inhibitor of HIV-1 replication. The advantage of this system is that, since MT-4 cells are stably transduced with a cDNA library, the anti-HIV-1 function of a candidate gene is not due to a perturbed cell physiology. This system has been successful in identifying CD14, CD63, and Brd4-CTD as regulators of HIV-1 replication [1,3,4], and more candidates are being analyzed. Among the candidates, SEC14L1a CTD appeared to be one of the relatively modest inhibitors of HIV-1 replication. However, of note, the SEC14L1a derivatives have not been identified in other genetic screening systems. These facts point that our T cell-based system is sensitive in detecting the modest anti-HIV-1 activity of a gene, and is a unique tool in the pursuit of HIV-1 regulatory factors to complete the HIV-1-host interactome.

SEC14L1a may affect the Golgi-mediated vesicular trafficking since SEC14L1a lowers the cell surface levels of cholinergic transporters [23]. However, we do not have any data to suggest that SEC14L1a and its derivatives affect the cell surface targeting of membrane proteins including CD4, CXCR4 and *Env*. These data suggest that SEC14L1a's effect on cholinergic receptor expression is specific, and that the CTD's ability to inhibit HIV-1 replication is independent from SEC14L1a's regulatory functions on vesicular trafficking. The action point of CTD1 and CTD2 was shown to be the late phase of the viral life cycle. Given that CTD1 and CTD2 did not inhibit the biogenesis and the cell surface targeting of *Gag* and *Env*, the major mechanism of CTD1 and CTD2 to inhibit HIV-1 replication was to reduce the infectivity of HIV-1 by limiting the *Env* incorporation onto the virion. Consistent with this idea, the viral infectivity of virions produced in CTDs-expressing cells was attenuated. Then, how do CTDs block the *Env* incorporation onto the virion? We detected a weak interaction between *Gag* and CTD1 or CTD2 by immuno-coprecipitation analysis. Thus, we speculate that the interaction between *Env* and *Gag* at the plasma membrane is interfered by *Gag*-CTDs interaction, resulting in the reduction of *Env* incorporation onto the virion.

The CTD1 was an inhibitor of HIV-1 replication. While the CTD1 negatively affected the *Env* incorporation onto the virion, it positively affected the HIV-1 production. These observations may be seemingly controversial. However, the SEC14L1a derivatives' effect on HIV-1 replication is a summation of their effects of on each step of the viral life cycle. Therefore, it is conceivable that CTD1 can serve as a negative regulator of HIV-1 replication as well as a positive and negative factor on distinct steps of the viral life cycle. These seemingly controversial findings may be in part due to the cells in which the biological functions of SEC14L1a derivatives were examined. The effect of SEC14L1a derivatives on HIV-1 replication was investigated in MT-4 cells, whereas those on the HIV-1 production and *Env* incorporation onto the virion were examined in 293T cells. Although the basic biological features are largely shared among different cell types, it is possible that the SEC14L1a derivatives may function slightly differently in MT-4 cells from 293T cells given that the intracellular distribution of SEC14L1a derivatives in MT-4 cells was not identical to that in 293T cells (Fig. 1E and 1F).

Elucidating the molecular mechanism underlying CTDs' activity not only provides a hint to understand how the HIV-1 virion actively uptakes *Env* through the *Gag-Env* interaction, but also leads to the development of a novel anti-retroviral drug that lowers the infectivity of the virus by preventing *Env* incorporation onto the virion. This is the strength of our T cell-based assay since CTDs inhibit HIV-1 replication specifically. In the previous study, we proposed that a small portion of Brd4 may serve as a therapeutic molecular target for HIV-1 infection, since the constitutive expression of Brd4-CTD limited HIV-1 replication specifically [3], akin to the SEC14L1a CTDs. However, it remains to be examined whether the SEC14L1a and Brd4 derivatives inhibit HIV-1 replication in primary HIV-1 target cells.

The genome-wide screening has potential caveats, including a cDNA bias and a cell line bias. A cDNA library is not a perfect representation of mRNA expressed in the cells from which the library is constructed. For example, the longer the mRNA, the less efficiently the full-length cDNA is synthesized. In fact, we isolated Brd4-CTD from the PBL cDNA library as a potent inhibitor of HIV-1 replication [3]. However, although Brd4 (approximately 5000 nt mRNA in length) is expressed in MT-4 cells, we were unable to recover Brd4-CTD from the MT-4 cDNA library [3]. This clearly demonstrates the cDNA bias in the genetic screening. A cDNA library derived from non-T cells does not contain genes specifically expressed in T cells. Thus, we have to explore many more cDNA libraries to completely cover the genetic diversity of human cells. The cDNA libraries isolated from long-term non-progressors of HIV-1-seropositive individuals or from elite controllers might be of particular interest, considering that a dominant innate HIV-1 resistance gene, such as CCR5 delta 32, may partly account for the slow progression of AIDS. Similarly, use of a particular cell line and/or virus strain may bias the results. MT-4 cells are positive for HTLV-1, and are able to support robust HIV-1 replication. MT-4 cells do not express CCR5, and are unable to support R5-tropic HIV-1 strains. What if other T cell lines and R5-tropic viral strains are used? What if we assay the same cDNA library in TZM-bl cells? We plan to address these issues in the future studies.

In conclusion, genome-wide genetic screening is a powerful tool for identifying the regulatory factors of HIV-1 replication and innate HIV-1 resistance factors that limit HIV-1 infection and AIDS progression. The HIV-1-host interactome should also reveal poten-

Please cite this article in press as: Urano E, et al. T cell-based functional cDNA library screening identified SEC14-like 1a carboxy-terminal domain as a negative regulator of human immunodeficiency virus replication. Vaccine (2009), doi:10.1016/j.vaccine.2009.07.084

tial therapeutic molecular targets that may be used to develop novel anti-AIDS drugs to tackle the emerging drug resistant viruses. However, the fact that different experimental systems often yield non-overlapping candidates suggests that we have to explore more experimental systems to fully understand the HIV-1-host interactome. Our T cell-based system provides an alternative tool for identifying novel HIV-1 regulatory factors, and should help us understand the HIV-1-host interaction in more detail.

Acknowledgements

This work was supported by the Japan Health Science Foundation, the Japanese Ministry of Health, Labor and Welfare, and the Japanese Ministry of Education, Culture, Sports, Science and Technology.

Conflict of interest: None.

References

[1] Kawano Y, Yoshida T, Hieda K, Aoki J, Miyoshi H, Koyanagi Y. A lentiviral cDNA library employing lambda recombination used to clone an inhibitor of human immunodeficiency virus type 1-induced cell death. J Virol 2004;78(20):11352–9.
[2] Valente ST, Goff SP. Inhibition of HIV-1 gene expression by a fragment of hnRNP U. Mol Cell 2006;23(4):597–605.
[3] Urano E, Kariya Y, Futahashi Y, Ichikawa R, Hamatake M, Fukazawa H, et al. Identification of the P-TEFb complex-interacting domain of Brd4 as an inhibitor of HIV-1 replication by functional cDNA library screening in MT-4 cells. FEBS Lett 2008;582(29):4053–8.
[4] Yoshida T, Kawano Y, Sato K, Ando Y, Aoki J, Miura Y, et al. A CD63 mutant inhibits T-cell tropic human immunodeficiency virus type 1 entry by disrupting CXCR4 trafficking to the plasma membrane. Traffic 2008;9(4):540–58.
[5] Zhou H, Xu M, Huang Q, Gates AT, Zhang XD, Castle JC, et al. Genome-scale RNAi screen for host factors required for HIV replication. Cell Host Microbe 2008;4(5):495–504.
[6] Brass AL, Dykxhoorn DM, Benita Y, Yan N, Engelman A, Xavier RJ, et al. Identification of host proteins required for HIV infection through a functional genomic screen. Science 2008;319(5865):921–6.
[7] Konig R, Zhou Y, Elleder D, Diamond TL, Bonamy GM, Irelan JT, et al. Global analysis of host-pathogen interactions that regulate early-stage HIV-1 replication. Cell 2008;135(1):49–60.
[8] Valente ST, Gilmartin GM, Mott C, Falkard B, Goff SP. Inhibition of HIV-1 replication by eIF3f. Proc Natl Acad Sci USA 2009;106(11):4071–8.
[9] Aiken C. Pseudotyping human immunodeficiency virus type 1 (HIV-1) by the glycoprotein of vesicular stomatitis virus targets HIV-1 entry to an endocytic pathway and suppresses both the requirement for Nef and the sensitivity to cyclosporin A. J Virol 1997;71(8):5871–7.
[10] Akari H, Uchiyama T, Fukumori T, Iida S, Koyama AH, Adachi A. Pseudotyping human immunodeficiency virus type 1 by vesicular stomatitis virus G protein does not reduce the cell-dependent requirement of vif for optimal infectivity: functional difference between Vif and Nef. J Gen Virol 1999;80(Pt 11):2945–9.
[11] Chazal N, Singer G, Aiken C, Hammarskjold ML, Rekosh D. Human immunodeficiency virus type 1 particles pseudotyped with envelope proteins that fuse at low pH no longer require Nef for optimal infectivity. J Virol 2001;75(8):4014–8.
[12] Komano J, Miyauchi K, Matsuda Z, Yamamoto N. Inhibiting the Arp2/3 complex limits infection of both intracellular mature vaccinia virus and primate lentiviruses. Mol Biol Cell 2004;15(12):5197–207.
[13] Goff SP. Knockdown screens to knockout HIV-1. Cell 2008;135(3):417–20.
[14] Urano E, Aoki T, Futahashi Y, Murakami T, Morikawa Y, Yamamoto N, et al. Substitution of the myristoylation signal of human immunodeficiency virus type 1 Pr55Gag with the phospholipase C-delta1 pleckstrin homology domain results in infectious pseudovirion production. J Gen Virol 2008;89(Pt 12):3144–9.
[15] Futahashi Y, Komano J, Urano E, Aoki T, Hamatake M, Miyauchi K, et al. Separate elements are required for ligand-dependent and–independent internalization of metastatic potentiator CXCR4. Cancer Sci 2007;98(3):373–9.
[16] Zufferey R, Dull T, Mandel RJ, Bukovsky A, Quiroz D, Naldini L, et al. Self-inactivating lentivirus vector for safe and efficient in vivo gene delivery. J Virol 1998;72(12):9873–80.
[17] Shimizu S, Urano E, Futahashi Y, Miyauchi K, Isogai M, Matsuda Z, et al. Inhibiting lentiviral replication by HEXIM1, a cellular negative regulator of the CDK9/cyclin T complex. AIDS 2007;21(5):575–82.
[18] Chinen K, Takahashi E, Nakamura Y. Isolation and mapping of a human gene (SEC14L), partially homologous to yeast SEC14, that contains a variable number of tandem repeats (VNTR) site in its 3' untranslated region. Cytogenet Cell Genet 1996;73(3):218–23.
[19] Howe AG, McMaster CR. Regulation of phosphatidylcholine homeostasis by Sec14. Can J Physiol Pharmacol 2006;84(1):29–38.
[20] Saito K, Tautz L, Mustelin T. The lipid-binding SEC14 domain. Biochim Biophys Acta 2007;1771(6):719–26.
[21] Mousley CJ, Tyeryar KR, Vincent-Pope P, Bankaitis VA. The Sec14-superfamily and the regulatory interface between phospholipid metabolism and membrane trafficking. Biochim Biophys Acta 2007;1771(6):727–36.
[22] Anantharaman V, Aravind L. The GOLD domain, a novel protein module involved in Golgi function and secretion. Genome Biol 2002;3(5), research0023.0021-0023.0027.
[23] Ribeiro FM, Ferreira LT, Marion S, Fontes S, Gomez M, Ferguson SS, et al. SEC14-like protein 1 interacts with cholinergic transporters. Neurochem Int 2007;50(2):356–64.

Please cite this article in press as: Urano E, et al. T cell-based functional cDNA library screening identified SEC14-like 1a carboxy-terminal domain as a negative regulator of human immunodeficiency virus replication. Vaccine (2009), doi:10.1016/j.vaccine.2009.07.084

Cancer Science
The official journal of the Japanese Cancer Association JCA

Dominant-negative derivative of EBNA1 represses EBNA1-mediated transforming gene expression during the acute phase of Epstein–Barr virus infection independent of rapid loss of viral genome

Yumi Kariya,[1,2] Makiko Hamatake,[1] Emiko Urano,[1] Hironori Yoshiyama,[3] Norio Shimizu[2] and Jun Komano[1,4]

[1]AIDS Research Center, National Institute of Infectious Diseases, Tokyo; [2]Department of Virology, Division of Medical Science, Medical Research Institute, Tokyo Medical and Dental University, Tokyo; [3]Research Center for Infection-associated Cancer, Institute for Genetic Medicine, Hokkaido University, Sapporo, Japan

(Received November 1, 2009/Revised November 30, 2009/Accepted December 6, 2009/Online publication February 2, 2010)

The oncogenic human herpes virus, the Epstein–Barr virus (EBV), expresses EBNA1 in almost all forms of viral latency. EBNA1 plays a major role in the maintenance of the viral genome and in the transactivation of viral transforming genes, including EBNA2 and latent membrane protein (LMP-1). However, it is unknown whether inhibition of EBNA1 from the onset of EBV infection disrupts the establishment of EBV's latency and transactivation of the viral oncogenes. To address this, we measured EBV infection kinetics in the B cell lines BALL-1 and BJAB, which stably express a dominant-negative EBNA1 (dnE1) fused to green fluorescent protein (GFP). The EBV genome was surprisingly unstable 1 week post-infection: the average loss rate of EBV DNA from GFP- and GFP-dnE1-expressing cells was 53.4% and 41.0% per cell generation, respectively, which was substantially higher than that of an 'established' *oriP* replicon (2–4%). GFP-dnE1 did not accelerate loss of the EBV genome, suggesting that EBNA1-dependent licensing of the EBV genome occurs infrequently during the acute phase of EBV infection. In the subacute phase, establishment of EBV latency was completely blocked in GFP-dnE1-expressing cells. In contrast, C/W promoter-driven transcription was strongly restricted in GFP-dnE1-expressing cells at 2 days post-infection. These data suggest that inhibition of EBNA1 from the onset of EBV infection is effective in blocking the positive feedback loop in the transactivation of viral transforming genes, and in eradicating the EBV genome during the subacute phase. Our results suggest that gene transduction of GFP-dnE1 could be a promising therapeutic and prophylactic approach toward EBV-associated malignancies. (*Cancer Sci* 2010; 101: 876–881)

The Epstein–Barr virus (EBV) is a risk factor in several malignant diseases including Burkitt's lymphoma and nasopharyngeal carcinoma.[1–4] The opportunistic B-cell lymphoma is becoming the major cause of death in AIDS patients in an era of highly active antiretroviral therapy (HAART), and EBV is associated with a significant portion of AIDS lymphoma cases.[5,6] Neither an EBV vaccine, nor specific antiviral agents against EBV are available; thus attention should be paid to the development of therapeutic agents against EBV.

EBV-encoded genes including EBNA1, EBNA2, and latent membrane protein (LMP-1) are potential molecular targets for the treatment of EBV-associated lymphomas because they play central roles in the process of malignant transformation.[7] We are interested in EBNA1 since it contributes to EBV oncogenesis in two ways: it supports the maintenance of the EBV genome in *cis* and enhances expression of viral oncogenes, including EBNA2 and LMP-1, in *trans*.[7–9] EBNA1 exerts its biological functions by binding to its cognate binding sites within the family of repeats (FR) and the dyad symmetry element (DS) located within the origin of replication (oriP) of EBV DNA. EBNA1 interacts with FR to enhance transcription from the viral C/W promoters (C/Wp) and to partition EBV DNA to daughter cells; and with DS to initiate DNA replication.[7–9]

Maintenance of the oriP replicon is stable once EBV latency has been established. The loss rate of established oriP plasmids is estimated at 2–4% per cell generation.[10,11] Interestingly, the loss rate of the oriP replicon is significantly higher in cells transiently transduced with oriP plasmids (>25% per cell generation) than in established cells.[12] In primary B cells, EBV DNA is lost rapidly within 2 days post-infection (~98.9%).[13] However, the loss rate of the EBV genome during a week post-infection in B cells remains to be quantified.

Upon EBV infection, the first viral genes expressed are the transactivators EBNA2 and EBNA-LP transcribed from Wp several hours after infection.[7] EBNA2 binds to the EBNA2-responsive elements and, in cooperation with EBNA-LP, enhances transcription from Cp, which leads to expression of all EBNA proteins, including EBNA1. EBNA1 binding to oriP activates C/Wp to boost viral latent gene expression, including the EBNAs and LMP-1. The viral gene transactivation positive feedback loop is established within a few days post-infection, and EBNA1 is one of the key factors that sustain this feedback loop during the acute phase of EBV infection.[14] In parallel, EBNA1 contributes to the establishment of the EBV genome as a licensed replicon. It may be possible to stop EBV infection by breaking the chain of EBNA1-dependent events and thus the EBV-mediated malignant transformation of infected cells. Previous studies have assessed the therapeutic potential of a dominant-negative derivative of EBNA1 (dnE1) in cells in which EBV latency was already established.[15,16] In this study, we critically assessed whether inhibition of EBNA1 limits the early stage of EBV infection in B cells. We provide evidence that expression of dnE1 strongly blocks the expression of virus-encoded oncogenes in acutely infected cells without accelerating EBV genome loss, and disrupts EBV latency in the subacute phase of EBV infection.

Materials and Methods

Cells. The 293T, EBV-negative Burkitt lymphoma cell line BJAB, EBV-positive Burkitt lymphoma cell line Daudi, EBV-transformed healthy donor-derived B lymphoblastoid cell line (B-LCL), and B acute lymphoblastic leukemia cell line BALL-1

[4]To whom correspondence should be addressed.
E-mail: ajkomano@nih.go.jp

doi: 10.1111/j.1349-7006.2009.01474.x

cells (kindly provided by Dr. Yokota, National Institute of Infectious Diseases, Tokyo, Japan) were maintained in RPMI-1640 medium (Sigma, St. Louis, MA, USA) supplemented with 10% fetal bovine serum (Japan Bioserum, Tokyo, Japan), 50 U/mL penicillin, 50 μg/mL streptomycin (Invitrogen, Tokyo, Japan), and incubated at 37°C in a humidified 5% CO_2 atmosphere.

Plasmids. The following primers were used to amplify dnE1 from p1160[17] by PCR: 5′-ACCGGTCTCGAGCAATTGCCA-CCATGCGGGGTCAGGGTGATGGAGG-3′ and 5′-GGATC-CTCGAGCGGCCGCTCACTCCTGCCCTTCCTCACC-3′. The GFP-dnE1 expression vector (pGD) was constructed by cloning the MfeI-XhoI fragment of the PCR product into the BglII-SalI sites of pEGFP-C1 (Clontech, Palo Alto, CA, USA). The MfeI and BglII sites were blunted with T7 RNA polymerase. The AgeI-BamHI fragment from pGD was cloned into the corresponding restriction sites of pCMMP eGFP[15,18] to generate pCMMP GFP-dnE1. The EBNA1 expression vector p1553, the FR-tk-luciferase reporter p985, and pLuciferase (pCMV-luc) have been described previously.[17–20]

Luciferase assay. The 293T cells, grown in 48-well plates, were co-transfected with the indicated plasmids using Lipofectamine 2000 according to the manufacturer's protocol (Invitrogen, Tokyo, Japan). Cells were replated in 96-well plates in triplicate at 2 h post-transfection. Luciferase activity was measured 48 h after transfection using the Steady-Glo Kit (Promega, Madison, WI, USA).

Murine leukemia virus (MLV) vector infection and cell sorting. MLV vectors were produced as described previously.[18] B cells (1×10^7 cells) were incubated with 2 mL of MLV preparation overnight at 4°C with continuous agitation. GFP-positive cells were collected using a FACS sorter (FACS Vantage; Becton Dickinson, San Jose, CA, USA) at 11 days post-infection.

Western blotting. Western blotting was performed as described previously.[21,22] The following reagents were used: anti-GFP (MsX Green Fluorescent Protein; Chemicon, Temecula, CA, USA) and Envision$^+$ Dual Link System-HRP (Dako, Glostrup, Denmark).

EBV infection and nucleic acid extraction. The EBV B95-8 strain was a generous gift from Dr Fujiwara's group at the National Research Institute for Child and Development (Tokyo, Japan). B cells (1×10^7 cells) were incubated with 100 μL of B95-8 EBV for 1 h at 37°C, and genomic DNA was extracted from half of the infected cells soon after infection (QIAamp DNA Mini Kit; Qiagen, Tokyo, Japan). At 15 h post-infection, half of the cells were washed once with PBS and incubated for 5 min in lysis buffer (10 mM Tris-HCl [pH7.4], 10 mM NaCl, 3 mM $MgCl_2$, and 0.5% NP-40). The nuclear fraction was collected by centrifugation for 5 min at 20.6 K × *g* (Kubota 3740; Kubota, Tokyo, Japan), and high molecular weight DNA was extracted (nuclear DNA). At 2 days post-infection and at later time points, high molecular weight DNA, or total RNA (PureLink Total RNA Blood Purification Kit; Invitrogen) was extracted from 1×10^6 or 3×10^6 cells, respectively, according to the manufacturer's protocol. After EBV infection, 10 μM aciclovir (Kayaku, Tokyo, Japan) was added to the culture medium. The production and infection of the recombinant EBV Akata strain carrying GFP and neomycin resistant genes has been described previously.[23] At 2 days post-infection, cells were plated at a density of 1×10^4 cells per well in a flat-bottomed 96-well plate, and cultured in a medium containing 1 mg/mL G418. The efficiency of EBV latency establishment was evaluated as percentage of wells positive for the emergence of G418-resistant cells at 2 to 3 weeks post-G418 selection.

Quantitative real-time PCR. Real-time PCR was performed as described previously; serial dilutions of positive controls were used as standards.[21] Amplifications were performed using the QuantiTect SYBR Green RT-PCR/PCR Kit (Qiagen), and the following primers: BamHI W repeat, 5′-GCCAGAGG-TAAGTGGACTTT-3′ and 5′-AGAAGCATGTATACTAAGC-CTCCC-3′; cyclophilin A (CYPA), 5′-CACCGCCACCATG-GTCAACCCCA-3′ and 5′-CCCGGGCCTCGAGCTTTCGAG-TTGTCCACAGTCAGCAATGG-3′; C/Wp, 5′-CCCTCGGA-CAGCTCCTAAG-3′ and 5′-CTTCACTTCGGTCTCCCCTA-3′; EBER1, 5′-AAAACATGCGGACCACCAGC-3′ and 5′-AG-GACCTACGCTGCCCTAGA-3′. The β-globin primers were described previously.[21] Following PCR amplification, the amplicons were separated in a 2% agarose gel, stained with ethidium bromide, and imaged with a Typhoon scanner (GE Healthcare Bio-Sciences; Piscataway, NJ, USA).

Results

Construction and functional verification of dnE1 fused to GFP. The carboxy half of EBNA1 serves as a functional dominant-negative inhibitor of EBNA1 that restricts the replication and maintenance of oriP plasmids as well as the EBNA1-dependent enhancement of transcription.[17,24] We used a dnE1 mutant encompassing amino acids 377 to 391 (the nuclear localization signal, NLS) and 451 to 641 (the DNA binding and dimerization domain) of EBNA1 (Fig. 1A).[17] To visualize the intracellular distribution of dnE1, we constructed the retroviral expression vector encoding GFP-dnE1. The expression of GFP-dnE1 was verified in transiently transfected 293T cells and stably transduced B cell lines using an MLV vector. To verify the function of GFP-dnE1, we conducted a reporter assay using a plasmid encoding the FR-tk-luciferase cassette. EBNA1 enhances expression of FR-tk-luciferase by binding to FR. If the GFP-dnE1 construct retains dnE1 function, co-expressing EBNA1 and GFP-dnE1 should reduce reporter activity. Luciferase activity was increased significantly upon EBNA1 expression by approximately 5.3-fold, consistent with previous findings (Fig. 1B, $P < 0.05$, two-tailed Student's *t*-test).[17] When GFP-dnE1 was co-expressed, the luciferase activity was decreased. The decrease in luciferase activity was proportional to the increase in GFP-dnE1 expression vector (Fig. 1B, maximum reduction: 22.3%, $P < 0.05$, two-tailed Student's *t*-test). This effect was not observed with GFP alone. In addition, CMV promoter-driven luciferase expression was unaffected by EBNA1, GFP-dnE1, and GFP, suggesting that the reduction in luciferase activity with GFP-dnE1 in the EBNA1/FR-tk-luciferase system is specific. These data indicate that GFP-dnE1 functions as an inhibitor of EBNA1.

Establishment of B cells constitutively expressing GFP-dnE1. To investigate the potential effect of GFP-dnE1 on EBV infection in B cells, we established BALL-1 and BJAB cells, which constitutively express GFP-dnE1, using an MLV vector. GFP was used as a control throughout this study. The distribution of GFP-dnE1 was examined by confocal microscopy, which revealed an even distribution of GFP throughout the cell. In contrast, the majority of GFP-dnE1was localized to the nucleus due to the presence of the NLS (Fig. 2A). Similar observations were made in BJAB and 293T cells (data not shown). We sorted the GFP- or GFP-dnE-expressing cells using a FACS sorter. To test the dose-dependent effect, we collected BALL-1 cell populations bearing high or low levels of GFP fluorescence, denoted as Hi and Lo, respectively. The expression of GFP and GFP-dnE1 was verified by Western blotting, which confirmed that GFP and GFP-dnE1 Hi cells had higher intensity signals than the GFP and GFP-dnE1 Lo cells (Fig. 2B). The rate of cell proliferation and the morphology of GFP-dnE1 cells were indistinguishable from those of GFP cells (Fig. 2A and data not shown).

Effect of GFP-dnE1 on the nuclear translocation of EBV DNA during the acute phase of EBV infection. To assess whether GFP-dnE1 could restrict the nuclear targeting of the EBV

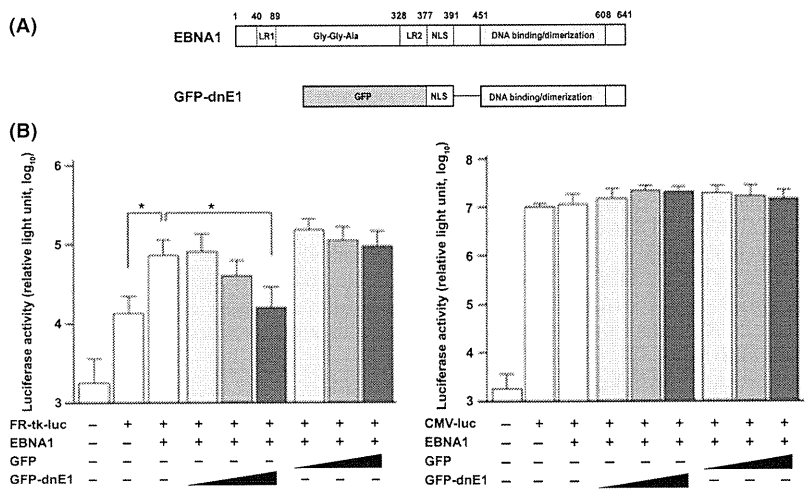

Fig. 1. Construction and functional characterization of a dominant-negative EBNA1 mutant (dnE1) fused to green fluorescent protein (GFP). (A) Structure of the EBNA1 protein and dnE1 used in this study. The linking regions (LR1 and LR2), the Gly-Gly-Ala repeat, the nuclear localization signal (NLS), and the DNA binding and dimerization domain are shown. GFP-dnE1 encodes the NLS and DNA binding and dimerization domain of EBNA1 fused to the C-terminus of GFP. (B) Repression of EBNA1-dependent transcriptional activation by GFP-dnE1. We transfected 293T cells in 48-well plates with 200 ng of FR-tk-luc or CMV-luc reporter, and 500 ng of EBNA1 expression vector, along with increasing amounts of GFP or GFP-dnE1 expression vector (20, 100, and 500 ng, respectively). $*P < 0.05$, two-tailed Student's *t*-test.

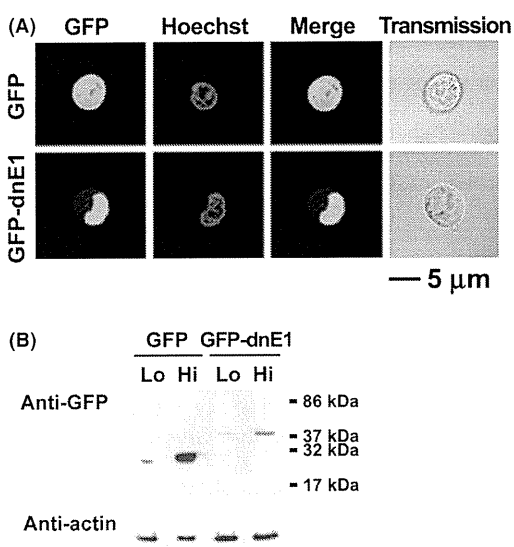

Fig. 2. Verification of stable green fluorescent protein (GFP)-dominant-negative EBNA1 (dnE1) expression in BALL-1 cells. (A) Distribution of GFP and GFP-dnE1 in BALL-1 cells was examined by confocal microscopy. Cells were imaged unfixed using a confocal microscope META 510 (Carl Zeiss, Tokyo, Japan). The green signal represents GFP fluorescence, and blue represents the Hoechst-stained nucleus. The bar represents 5 μm; magnification, ×630. (B) GFP or GFP-dnE1 expression in stably transduced BALL-1 cells was examined by Western blot analysis using an anti-GFP antibody. Protein lysates from 5×10^5 cells were loaded for each sample, except GFP Hi cells (5×10^4). The molecular weight marker is shown on the right.

genome after infection, we measured the amount of EBV DNA recovered from cells immediately after infection (representing the amount of EBV attached to cells) and the amount of EBV DNA that had migrated into the nucleus at 1 day post-infection. We isolated the nuclear fraction to exclude EBV DNA that failed to enter the nucleus. The number of EBV DNA molecules per cell was estimated by real-time PCR, which targeted the BamHI W repeat, in 10 ng of genomic DNA. We estimated the number of EBV DNA per cell given that a single cell contains approximately 10 pg of genomic DNA, and an EBV DNA has 10 copies of BamHI W repeats on average. The nuclear targeting efficiencies of EBV DNA were as follows: BALL-1 GFP cells, 43.3–108.6%; GFP-dnE1 cells, 46.9–65.6%; BJAB GFP cells, 37.4%; GFP-dnE1 cells, 35.0% (Table 1). These data suggested that the effect of GFP-dnE1 on the nuclear targeting of EBV DNA should be assessed more sensitively in BALL-1 and BJAB cell systems than in primary B cells because the nuclear targeting efficiency of EBV DNA in primary B cells is extremely inefficient (~1.1%).[13] In our experimental systems, the nuclear targeting efficiencies of EBV DNA in GFP-dnE1-expressing cells were similar to those in GFP-expressing cells. In addition, the dose-dependency of GFP-dnE1 was not observed in BALL-1 cells (Table 1). These data suggest that the nuclear targeting efficiency of EBV DNA was not restricted by the presence of GFP-dnE1 in B cells upon EBV infection.

Effect of GFP-dnE1 on the rate of loss of EBV DNA during the acute phase of EBV infection. To examine the effect of GFP-dnE1 on the rate of loss (ROL) of EBV DNA during the acute phase of viral infection, we monitored the EBV DNA copy number from day 2 to day 5 or day 6 post-infection, by real-time PCR, which detects the viral genome in both linear and circular configurations (Table 1). The ROL was estimated as the percentage reduction of EBV DNA per cell generation, considering that the cell doubling time is 24 h, and the kinetics of viral genome loss follows an exponential decay. The ROL in GFP-dnE1-expressing cells (19.2–85.9% per cell generation) was similar to GFP-expressing cells (20.5–79.4% per cell generation) in both BALL-1 and BJAB cells. In addition, there was no detectable dose-dependent effect of GFP-dnE1 in BALL-1 cells (Table 1 and Fig. 3). The averages ± SEs of ROL in GFP- and GFP-dnE1-expressing cells from six independent measurements in BALL-1 cells were 37.7 ± 10.7% and 25.7 ± 6.5% per cell generation, respectively (data not shown), which was substantially higher than the rate of loss of an established oriP replicon (2–4%).[10,11] These results reflect the precipitous loss of oriP plas-

doi: 10.1111/j.1349-7006.2009.01474.x

Table 1. The kinetics of EBV DNA in the acute phase of EBV infection

Cell	Copy number of EBV DNA per cell at the indicated day†				Nuclear transport (%‡)	Rate of loss of EBV DNA (% per cell generation§)
Expt 1						
BALL-1	Day 0	Day 1	Day 2	Day 5		
GFP Hi	20.38	11.92	3.57	0.01¶	58.5	85.9
GFP Lo	17.26	11.68	3.21	0.56	67.7	44.1
GFP-dnE1 Hi	23.02	10.79	3.30	0.30	46.9	54.9
GFP-dnE1 Lo	18.83	12.36	1.46	0.53	65.6	28.7
BJAB	Day 0	Day 1	Day 2	Day 5		
GFP	155.1	58.8	5.38	0.06	37.4	77.7
GFP-dnE1	64.6	37.4	5.69	0.05	58.0	79.4
Expt 2						
BALL-1	Day 0	Day 1	Day 2	Day 6		
GFP Hi	16.33	17.73	11.10	4.74	108.6	19.2
GFP Lo	17.35	7.51	8.75	1.13	43.3	40.1
GFP-dnE1 Hi	18.46	8.71	8.95	3.38	47.2	21.6
GFP-dnE1 Lo	14.14	7.05	6.97	2.79	49.9	20.5

†Nuclear DNA was used for day 1 data. ‡Estimated from day 0 and day 1 data. §Estimated from day 2 and day 5 or day 6 data with the exponential decay. ¶Below the limit of detection. dnE1, dominant-negative EBNA1; EBV, Epstein–Barr virus; GFP, green fluorescent protein.

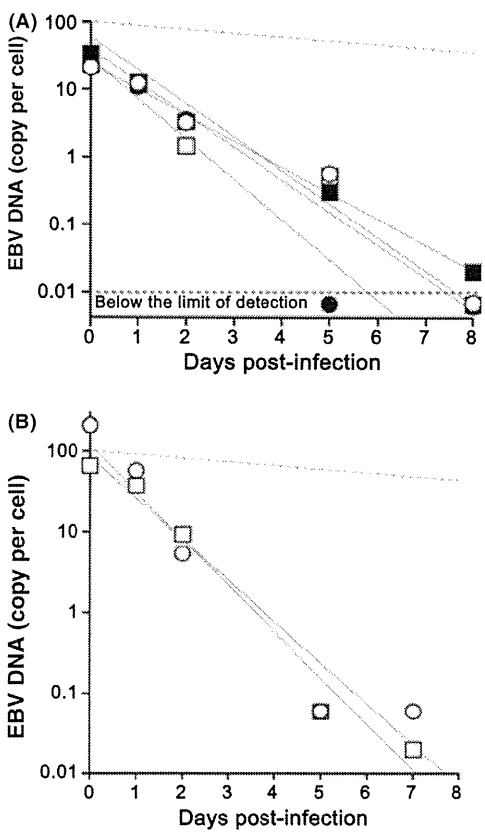

Fig. 3. Kinetics of Epstein–Barr virus (EBV) DNA loss during the acute phase of EBV infection. (A) Representative data from BALL-1 cells (Expt. 1 in Table 1) is shown. The filled squares, open squares, filled circles, and open circles represent GFP Hi, GFP Lo, GFP-dnE1 Hi, and GFP-dnE1 Lo, respectively. The limit of detection was below 0.01 (dashed line). The gray lines represent an approximation to the exponential decay. The dashed gray line represents the 4% rate of loss per cell generation. (B) Representative data from BJAB cells shown in Table 1. The circles and squares represent GFP and GFP-dnE1, respectively. Please see Table 1 for the detailed analysis.

mids (26–37%) in transiently transfected non-B cells.[12] The data suggest that GFP-dnE1 is unable to accelerate the ROL in the acute phase of EBV infection in B cells, presumably because the EBV genome is not established as an EBNA1-dependent stable licensed replicon. It should be noted that this is the first time that quantitative ROL data has been obtained by introducing the oriP replicon into B cells via EBV infection, which is an approach that does not confer any selective advantage on the infected cells.

Effect of GFP-dnE1 on efficiency of establishment of EBV latency. Cells infected with recombinant EBV_3 carrying the neomycin resistance gene, were seeded at 5×10^3 cells per well into a 96-well plate, and the efficiency of the establishment of EBV latency was assessed as the percentage of wells positive for the emergence of G418-resistant cells. G418-resistant cells appeared in BJAB, Daudi, parental BALL-1, and BALL-1 GFP cells at 56–100% efficiencies. In sharp contrast, G418-resistant cells were absent from GFP-dnE1-expressing BALL-1 cells (Table 2). These data clearly suggest that, although the ROL during the acute phase of EBV infection was not enhanced by GFP-dnE1, GFP-dnE1 was able to block the establishment of EBV latency completely during the subacute phase of EBV infection.

Effect of GFP-dnE1 on EBV-encoded latent gene expression. EBV gene expression was tested at 2 days post-infection by quantitative RT-PCR. We focused on the C/Wp activity because it expresses key viral transactivators including EBNA1, -2, -3s, and -LP to boost viral transforming gene expression. We detected C/Wp-driven transcripts in GFP Hi BALL-1 cells as expected. Conversely, C/Wp-driven transcripts were undetectable in GFP-dnE1 Hi and Lo BALL-1 cells, although these cells retained similar EBV DNA levels to GFP-expressing cells (Fig. 4 and Table 3). The Cp-driven transcript was under the limit of detection by RT-PCR, suggesting that the Wp is predominantly activated at the early phase of EBV infection consistent with previous findings.[7] Inhibition of viral gene transcription was not observed in the RNA polymerase III-driven transcript EBER1,[25] and cyclophilin A mRNA levels were similar between GFP- and GFP-dnE1-expressing cells (Fig. 4 and Table 3). This indicates that the effect of GFP-dnE1 on C/Wp activity is specific, and uncovers an active role of EBNA1 in supporting transactiva-

Table 2. The establishment efficiency of EBV latency

Cell	Emergence of G418-resistant cells†	
BJAB	100%	(6/6)
Daudi	100%	(10/10)
BALL-1		
Parental	56%	(5/9)
GFP Hi	67%	(2/3)
GFP-dnE1 Hi	0%	(0/6)
GFP-dnE1 Lo	0%	(0/6)

†Percentage of wells positive for G418-resistant cells over the number of tested wells from 96-well plates indicated in the bracket. Shown are the sum of two independent experiments. dnE1, dominant-negative EBNA1; EBV, Epstein–Barr virus; GFP, green fluorescent protein.

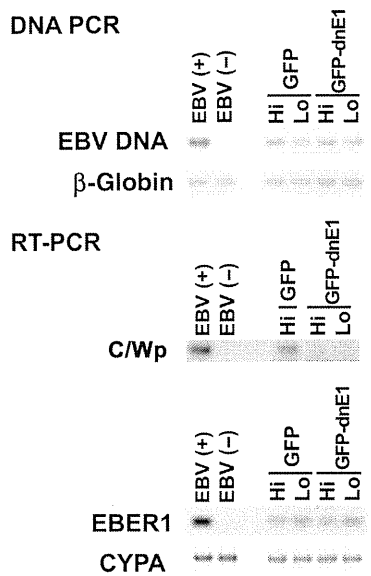

Fig. 4. PCR-based analysis of Epstein–Barr virus (EBV) gene expression. The effect of green fluorescent protein (GFP)-dominant-negative EBNA1 (dnE1) on the loss of EBV DNA (DNA PCR, upper panels) and transcription of the C/W promoter-driven transcript (C/Wp), EBER1, and cyclophilin A (CYPA; RT-PCR, lower panels) in BALL-1 cells at 2 days post-infection were examined. EBV-transformed B-lymphoblastoid cell line (B-LCL) and BJAB cells, denoted as EBV(+) and EBV(−), were used as positive and negative controls for viral DNA and RNA shown, respectively. β-Globin and CYPA were used as controls.

Table 3. Quantification of EBV transcripts in BALL-1 cells by real-time PCR at 2 days post-infection

BALL-1 cells		W1/2 exon (copies†)	EBER1 (copies‡)	CYPA (copies‡)
GFP	Hi	2.2	2.8×10^2	1.4×10^6
	Lo	NT§	0.8×10^2	1.0×10^6
GFP-dnE1	Hi	BLD¶	3.3×10^2	1.3×10^6
	Lo	BLD¶	1.2×10^2	1.5×10^6

†Copies per 13–14 ng total cellular RNA. ‡Copies per 200 ng total cellular RNA. §Not tested. ¶Below the limit of detection. CYPA, cyclophilin A; dnE1, dominant-negative EBNA1; EBV, Epstein–Barr virus; GFP, green fluorescent protein.

tion from C/Wp. Taken together, these results show that inhibition of EBNA1 functions strongly restricts EBV-encoded transforming gene expression and, although there is no detectable effect on the ROL of EBV DNA at the acute phase of viral infection, it blocks the establishment of EBV latency during the subacute phase.

Discussion

This is the first report describing the effect of EBNA1 inhibition from the onset of EBV infection in B cells. Unexpectedly, the dnE1 was unable to accelerate the ROL during the acute phase of EBV infection since dnE1 enhanced the loss of the oriP plasmid in the transient transfection assays.[10,11] In the subacute phase of EBV infection, the establishment of EBV latency was potently blocked by dnE1. In addition, we observed a strong repressive effect of dnE1 on the EBNA1-dependent enhancement of viral gene transcription from C/Wp during the early phase of EBV infection, similar to the transient transfection assays.[17] These data suggest that viral oncogene expression depends heavily on EBNA1 during the acute phase of viral infection, and that EBNA1 contributes little to EBV genome maintenance during this period. The results emphasize that an EBNA1 inhibitor should serve as an attenuator of viral oncogene expression since activation of C/Wp is the 'root' event of the positive feedback loop involved in the transactivation of viral transforming gene expression. In this regard, the EBNA1 inhibition approach could be superior to LMP-1 or EBNA2 inhibition.

If EBNA1 binding to oriP is essential for both the enhancement of viral gene transcription and for genome maintenance, what mechanism prevents dnE1 from affecting the ROL during the acute phase of EBV infection? It is likely that maintenance of the oriP replicon immediately after its introduction into cells is less efficient than in cells harboring an 'established' oriP replicon as an autonomously replicating plasmid. The ROL of an established oriP replicon is 2–4% per cell generation.[10,11] In contrast, our data from the EBV/B cell-based assay gave an average ROL of 26–38% during the week post-infection (acute phase of EBV infection). In agreement with our findings, it is reported that a transiently transduced oriP replicon is lost from cells at 26–37% per cell generation 1–2 weeks post-plasmid transduction.[12] These data indicate that maintenance of the oriP replicon is largely EBNA1-independent immediately after its introduction into cells, regardless of whether the route of introduction is by transfection or EBV infection. In other words, the establishment of EBV latency should be a rare epigenetic event. The data also suggest that the artificial minichromosome approach may be relevant in understanding EBV genome behavior.[12]

Our study suggests that gene therapy using GFP-dnE1 is an attractive approach, not only for therapeutics, but also for prophylactic interventions of EBV-associated malignancies. For example, in peripheral blood stem cell transplantation (PBSCT), GFP-dnE1 transduction into $CD34^+$ cells should protect the differentiated B cells from EBV infection, thus preventing the genesis of EBV-associated B cell lymphomas. We will attempt to prove this hypothesis using a small animal model in future studies.[26] Additionally, EBNA1 is a potential molecular target for developing a small molecular-weight EBV inhibitor as mentioned previously.[14,15] The advantages of EBNA1-inhibitor development are that the biological assay system is already established and the X-ray crystal structure of the DNA-bound EBNA1 DNA binding and dimerization domain is known, which means that computer-aided drug design technology can be immediately applied. Although EBV is associated with various malignancies, preventive and therapeutic measures against EBV infection have not been developed. We believe that an anti-EBV agent, such as an EBNA1 inhibitor, would have an enormous impact in the medical field due to the substantial number of patients with EBV-associated malignancies.

doi: 10.1111/j.1349-7006.2009.01474.x

Acknowledgments

We thank Drs Kenichi Imadome and Shigeyoshi Fujiwara for reagents. We also thank Dr Bill Sugden for critically reading the manuscript. This work was supported by the Japan Health Science Foundation, the Ministry of Health, Labor and Welfare of Japan, and the Ministry of Education, Culture, Sports, Science and Technology of Japan.

Disclosure Statement

The authors have no conflict of interest.

References

1 Thompson MP, Kurzrock R. Epstein–Barr virus and cancer. *Clin Cancer Res* 2004; **10**: 803–21.
2 Rickinson AB, Kieff E. Epstin–Barr virus. In: Knipe DM, Howley PM, eds. *Fields Virology*, 5th edn, vol. 2. Philadelphia: Lippincott Williams & Wilkins, 2007; 2655–700.
3 Klein E, Kis LL, Klein G. Epstein–Barr virus infection in humans: from harmless to life endangering virus-lymphocyte interactions. *Oncogene* 2007; **26**: 1297–305.
4 Snow AL, Martinez OM. Epstein–Barr virus: evasive maneuvers in the development of PTLD. *Am J Transplant* 2007; **7**: 271–7.
5 Besson C, Goubar A, Gabarre J *et al.* Changes in AIDS-related lymphoma since the era of highly active antiretroviral therapy. *Blood* 2001; **98**: 2339–44.
6 Carbone A, Cesarman E, Spina M, Gloghini A, Schulz TF. HIV-associated lymphomas and gamma-herpesviruses. *Blood* 2009; **113**: 1213–24.
7 Kieff E, Rickinson AB. Epstin–Barr virus and its replication. In: Knipe DM, Howley PM, eds. *Fields Virology*, 5th edn, vol. 2. Philadelphia: Lippincott Williams & Wilkins, 2007; 2603–54.
8 Lindner SE, Sugden B. The plasmid replicon of Epstein–Barr virus: mechanistic insights into efficient, licensed, extrachromosomal replication in human cells. *Plasmid* 2007; **58**: 1–12.
9 Wang J, Sugden B. Origins of bidirectional replication of Epstein–Barr virus: models for understanding mammalian origins of DNA synthesis. *J Cell Biochem* 2005; **94**: 247–56.
10 Kirchmaier AL, Sugden B. Plasmid maintenance of derivatives of oriP of Epstein–Barr virus. *J Virol* 1995; **69**: 1280–3.
11 Sugden B, Warren N. Plasmid origin of replication of Epstein–Barr virus, oriP, does not limit replication in cis. *Mol Biol Med* 1988; **5**: 85–94.
12 Leight ER, Sugden B. Establishment of an oriP replicon is dependent upon an infrequent, epigenetic event. *Mol Cell Biol* 2001; **21**: 4149–61.
13 Hurley EA, Thorley-Lawson DA. B cell activation and the establishment of Epstein–Barr virus latency. *J Exp Med* 1988; **168**: 2059–75.
14 Altmann M, Pich D, Ruiss R, Wang J, Sugden B, Hammerschmidt W. Transcriptional activation by EBV nuclear antigen 1 is essential for the expression of EBV's transforming genes. *Proc Natl Acad Sci U S A* 2006; **103**: 14188–93.
15 Kennedy G, Komano J, Sugden B. Epstein–Barr virus provides a survival factor to Burkitt's lymphomas. *Proc Natl Acad Sci U S A* 2003; **100**: 14269–74.
16 Nasimuzzaman M, Kuroda M, Dohno S *et al.* Eradication of Epstein–Barr virus episome and associated inhibition of infected tumor cell growth by adenovirus vector-mediated transduction of dominant-negative EBNA1. *Mol Ther* 2005; **11**: 578–90.
17 Kirchmaier AL, Sugden B. Dominant-negative inhibitors of EBNA-1 of Epstein–Barr virus. *J Virol* 1997; **71**: 1766–75.
18 Komano J, Miyauchi K, Matsuda Z, Yamamoto N. Inhibiting the Arp2/3 complex limits infection of both intracellular mature vaccinia virus and primate lentiviruses. *Mol Biol Cell* 2004; **15**: 5197–207.
19 Aiyar A, Sugden B. Fusions between Epstein–Barr viral nuclear antigen-1 of Epstein–Barr virus and the large T-antigen of simian virus 40 replicate their cognate origins. *J Biol Chem* 1998; **273**: 33073–81.
20 Middleton T, Sugden B. EBNA1 can link the enhancer element to the initiator element of the Epstein–Barr virus plasmid origin of DNA replication. *J Virol* 1992; **66**: 489–95.
21 Urano E, Kariya Y, Futahashi Y *et al.* Identification of the P-TEFb complex-interacting domain of Brd4 as an inhibitor of HIV-1 replication by functional cDNA library screening in MT-4 cells. *FEBS Lett* 2008; **582**: 4053–8.
22 Shimizu S, Urano E, Futahashi Y *et al.* Inhibiting lentiviral replication by HEXIM1, a cellular negative regulator of the CDK9/cyclin T complex. *AIDS* 2007; **21**: 575–82.
23 Kanda T, Yajima M, Ahsan N, Tanaka M, Takada K. Production of high-titer Epstein–Barr virus recombinants derived from Akata cells by using a bacterial artificial chromosome system. *J Virol* 2004; **78**: 7004–15.
24 Mackey D, Sugden B. The linking regions of EBNA1 are essential for its support of replication and transcription. *Mol Cell Biol* 1999; **19**: 3349–59.
25 Howe JG, Shu MD. Epstein–Barr virus small RNA (EBER) genes: unique transcription units that combine RNA polymerase II and III promoter elements. *Cell* 1989; **57**: 825–34.
26 Yajima M, Imadome K, Nakagawa A *et al.* A new humanized mouse model of Epstein–Barr virus infection that reproduces persistent infection, lymphoproliferative disorder, and cell-mediated and humoral immune responses. *J Infect Dis* 2008; **198**: 673–82.

Bioorganic & Medicinal Chemistry 18 (2010) 6771–6775

Contents lists available at ScienceDirect

Bioorganic & Medicinal Chemistry

journal homepage: www.elsevier.com/locate/bmc

Peptidic HIV integrase inhibitors derived from HIV gene products: Structure–activity relationship studies

Shintaro Suzuki [a], Kasthuraiah Maddali [b], Chie Hashimoto [a], Emiko Urano [c], Nami Ohashi [a], Tomohiro Tanaka [a], Taro Ozaki [a], Hiroshi Arai [a], Hiroshi Tsutsumi [a], Tetsuo Narumi [a], Wataru Nomura [a], Naoki Yamamoto [c,d], Yves Pommier [b], Jun A. Komano [c], Hirokazu Tamamura [a,*]

[a] Institute of Biomaterials and Bioengineering, Tokyo Medical and Dental University, Chiyoda-ku, Tokyo 101-0062, Japan
[b] Laboratory of Molecular Pharmacology, Center for Cancer Research, National Cancer Institute, National Institutes of Health, Bethesda, MD 20892-4255, USA
[c] AIDS Research Center, National Institute of Infectious Diseases, Shinjuku-ku, Tokyo 162-8640, Japan
[d] Department of Microbiology, Yong Loo Lin School of Medicine, National University of Singapore, Singapore 117597, Singapore

ARTICLE INFO

Article history:
Received 28 June 2010
Revised 17 July 2010
Accepted 20 July 2010
Available online 25 July 2010

Keywords:
HIV integrase
Inhibitory peptide
Glu-Lys pairs
Ala-scan

ABSTRACT

Structure–activity relationship studies were conducted on HIV integrase (IN) inhibitory peptides which were found by the screening of an overlapping peptide library derived from HIV-1 gene products. Since these peptides located in the second helix of Vpr are considered to have an α-helical conformation, Glu-Lys pairs were introduced into the *i* and *i* + 4 positions to increase the helicity of the lead compound possessing an octa-arginyl group. Ala-scan was also performed on the lead compound for the identification of the amino acid residues responsible for the inhibitory activity. The results indicated the importance of an α-helical structure for the expression of inhibitory activity, and presented a binding model of integrase and the lead compound.

1. Introduction

Highly active anti-retroviral therapy (HAART), which involves a combination of two or three agents from two categories, reverse transcriptase inhibitors and protease inhibitors, has brought us remarkable success in the clinical treatment of HIV-infected and AIDS patients.[1] However, it has been accompanied by serious clinical problems including the emergence of viral strains with multidrug resistance (MDR), considerable adverse effects and nonetheless high costs. As a result, new categories of anti-HIV agents operating with mechanisms of action different from those of the above inhibitors are sought. HIV-1 integrase (IN) is a critical enzyme for the stable infection of host cells since it catalyzes the insertion of viral DNA into the genome of host cells, by means of strand transfer and 3′-end processing reactions and thus it is an attractive target for the development of anti-HIV agents. Recently, the first IN inhibitor, raltegravir (Merck),[2] has appeared in a clinical setting. It is assumed that the activity of IN must be negatively regulated during the translocation of the viral DNA from the cytoplasm to the nucleus to prevent auto-integration. The virus, as well as the host cells, must encode mechanism(s) to prevent auto-integration since the regulation of IN activity is critical for the virus to infect cells.[3] By screening a library of overlapping peptides derived from HIV-1 SF2 gene products we have found three Vpr-derived peptides, **1**, **2** and **3**, which possess significant IN inhibitory activity, indicating that IN inhibitors exist in the viral pre-integration complex (PIC).[4] The above inhibitory peptides, **1**, **2** and **3**, are consecutive overlapping peptides (Fig. 1). Compounds **4** and **5** are 12- and 18-mers from the original Vpr-sequence with the addition of an octa-arginyl group[5] into the C-terminus for cell membrane permeability, respectively. Compounds **4** and **5** have IN inhibitory activity and anti-HIV activity. Here, we report structure–activity relationship studies on these lead compounds for the development of more potent IN inhibitors.

2. Results and discussion

To determine which lead compound is most suitable for further experiments, five peptides **6–10**, which were elongated by one amino acid starting with compound **4** and extended ultimately to **5**, were synthesized (Fig. 2). Judging by the 3′-end processing and strand transfer reactions in vitro,[6] these peptides **4–10** had similar inhibitory potencies (Table 1). As a result, we concluded that 12 amino acid residues derived from the original Vpr-sequence are of sufficient for IN inhibitory activity, and any peptide among **4–10** is a suitable lead.

* Corresponding author.
E-mail address: tamamura.mr@tmd.ac.jp (H. Tamamura).

0968-0896/$ - see front matter © 2010 Elsevier Ltd. All rights reserved.
doi:10.1016/j.bmc.2010.07.050

1 AGVEAIIRILQQLLF
2 IIRILQQLLFIHFRI
3 LQQLLFIHFRIGCQH
4 Ac-LQQLLFIHFRIG-RRRRRRRR-NH_2
5 Ac-EAIIRILQQLLFIHFRIG-RRRRRRRR-NH_2

Figure 1. Amino acid sequences of compounds **1–5**. Compounds **1–3** are consecutive overlapping peptides with free N-/C-terminus. These were found by the IN inhibitory screening of a peptide library derived from HIV-1 gene products. Compounds **4** and **5** are cell penetrative leads of IN inhibitors.

4 Ac-LQQLLFIHFRIG-RRRRRRRR-NH_2
6 Ac-ILQQLLFIHFRIG-RRRRRRRR-NH_2
7 Ac-RILQQLLFIHFRIG-RRRRRRRR-NH_2
8 Ac-IRILQQLLFIHFRIG-RRRRRRRR-NH_2
9 Ac-IIRILQQLLFIHFRIG-RRRRRRRR-NH_2
10 Ac-AIIRILQQLLFIHFRIG-RRRRRRRR-NH_2
5 Ac-EAIIRILQQLLFIHFRIG-RRRRRRRR-NH_2

Figure 2. Amino acid sequences of compounds **6–10**, which are elongated by one amino acid from compound **4** to **5**.

Table 1
IC_{50} values of compounds **4–10** toward the 3′-end processing and strand transfer reactions catalyzed by HIV-1 IN

Compound	IC_{50} (μM)	
	3′-End processing	Strand transfer
4	0.13 ± 0.02	0.06 ± 0.01
5	0.09 ± 0.01	0.04 ± 0.01
6	0.10 ± 0.01	0.07 ± 0.01
7	0.13 ± 0.02	0.11 ± 0.01
8	0.26 ± 0.04	0.11 ± 0.03
9	0.11 ± 0.01	0.07 ± 0.01
10	0.08 ± 0.01	0.05 ± 0.01

Structural analysis showed that the Vpr-derived peptides, **1**, **2** and **3**, are located in the second helix of Vpr and were thus considered to have an α-helical conformation.[7] Compound **5** was adopted as a lead for the development of compounds with an increase in α-helicity since a longer peptide is likely to form a more stable α-helical structure than a shorter one. Initially, Glu (E) and Lys (K) were introduced in pairs into compound **5** at the i and $i+4$ positions. In general, such disposition of Glu-Lys pairs at i and $i+4$ positions is considered to cause an increase in α-helicity due to formation of an ionic interaction of a β-carboxy group of Glu and an ε-amino group of Lys. Several analogs of **5** with Glu-Lys pairs were synthesized by Fmoc-solid phase peptide synthesis (Fig. 3). In the inhibitory assay against the 3′-end processing and strand transfer reactions catalyzed by HIV-1 IN in vitro, compounds **11** and **15** showed more potent inhibitory activities than **5** (Table 2). Substitution of Glu-Lys for His^{14}-Gly^{18} or Ile^{3}-Leu^{7} caused no decrease in IN inhibitory activity but a significant increase in activity, suggesting that Ile^3, Leu^7, His^{14} and Gly^{18} are not indispensable for activity. Substitution of Glu-Lys for Ala^2-Ile^6 or Gln^9-Ile^{13} caused a slight decrease in IN inhibitory activity against the 3′-end processing and strand transfer reactions (compounds **12** and **13**), indicating that Ala^2 and/or Ile^6, and Gln^9 and/or Ile^{13} are partly required for activity. Substitution of Glu-Lys for Ile^4-Gln^8 caused a 2–4-fold decrease in IN inhibitory activity against the 3′-end processing and strand transfer reactions (compound **14**), showing that Ile^4 and/or Gln^8 are essential for activity. Substitution of Glu-Lys for Leu^{11}-Phe^{15} caused an eightfold decrease in IN inhibitory activity against the 3′-end processing reaction and a 1.5-fold decrease in IN inhibitory activity against the strand transfer reaction (compound **16**), indicating that Leu^{11} and/or Phe^{15} are indispensable for activity, especially for inhibition against 3′-end processing. Compound **17** has two substitutions of Glu-Lys for His^{14}-Gly^{18} and for Ala^2-Ile^6, which are common to compounds **11** and **12**, respectively. A twofold decrease in both IN inhibitory activities of compound **17** is mostly due to the substitution for Ala^2-Ile^6 common to **12**, although **17** is slightly less active than **12** in both IN inhibitory assays.

1 5 10 15
5 Ac-EAIIRILQQLLFIHFRIG-RRRRRRRR-NH_2
11 Ac-EAIIRILQQLLFI*E*FRI*K*-RRRRRRRR-NH_2
12 Ac-E*E*IIR*K*LQQLLFIHFRIG-RRRRRRRR-NH_2
13 Ac-EAIIRILQ*E*LLF*K*HFRIG-RRRRRRRR-NH_2
14 Ac-EAI*E*RIL*K*QLLFIHFRIG-RRRRRRRR-NH_2
15 Ac-EA*E*IRI*K*QQLLFIHFRIG-RRRRRRRR-NH_2
16 Ac-EAIIRILQQL*E*FIH*K*RIG-RRRRRRRR-NH_2
17 Ac-E*E*IIR*K*LQQLLFI*E*FRI*K*-RRRRRRRR-NH_2

Figure 3. Amino acid sequences of compounds **11–17**, into which Glu-Lys pairs have been introduced.

Table 2
IC_{50} values of compounds **5** and **11–17** toward the 3′-end processing and strand transfer reactions catalyzed by HIV-1 IN

Compound	IC_{50} (μM)	
	3′-End processing	Strand transfer
5	0.09 ± 0.01	0.04 ± 0.01
11	0.05 ± 0.01	0.01 ± 0.001
12	0.12 ± 0.01	0.047 ± 0.01
13	0.14 ± 0.02	0.065 ± 0.01
14	0.23 ± 0.03	0.15 ± 0.002
15	0.04 ± 0.01	0.031 ± 0.01
16	0.71 ± 0.21	0.06 ± 0.004
17	0.18 ± 0.06	0.08 ± 0.02

Anti-HIV activity of these compounds was assessed by an MT-4 Luc system, in which MT-4 cells were stably transduced with the firefly luciferase expression cassette by a murine leukemia viral vector. MT-4 Luc cells constitutively express high levels of luciferase. HIV-1 infection significantly reduces luciferase expression due to the high susceptibility of MT-4 cells to HIV-1 infection. Protection of MT-4 Luc cells from HIV-1-induced cell death maintains the luciferase signals at high levels. In addition, the cytotoxicity of test compounds can be evaluated by a decrease of luciferase signals in these MT-4 Luc systems. The parent compound **5** showed significant anti-HIV activity at concentrations above 1.25 μM, as reported previously (Fig. 4).[4] Compound **15** showed a significant inhibitory effect against HIV-1 replication, and is thus comparable to compound **5**. Compounds **11**, **14** and **16** also displayed weak antiviral effects at concentrations of 2.5 and 5.0 μM and compounds **12**, **13** and **17** failed to show any significant anti-HIV activity. These results suggest that there is a positive correlation between IN inhibitory activity and anti-HIV activity of the compounds. None of these compounds showed significant cytotoxic effects at concentrations below 5.0 μM.

The structures of compounds **5** and **11–17** were assessed by CD spectroscopy. Because the aqueous solubility of these peptides is not high the peptides were dissolved in 0.1 M phosphate buffer, containing 50% MeOH at pH 5.6. The CD spectra suggest that the parent compound **5**, which has no Glu-Lys pair, forms a typical α-helical structure, and the other compounds, with the exception of **11** and **15**, form α-helical structures similarly (Fig. 5). The order of strength of α-helicity is **12**, **16** > **14** > **17** > **5** > **13**. Compounds **11** and **15** have no characteristic pattern, although IN inhibitory activities of both compounds are superior to that of the parent

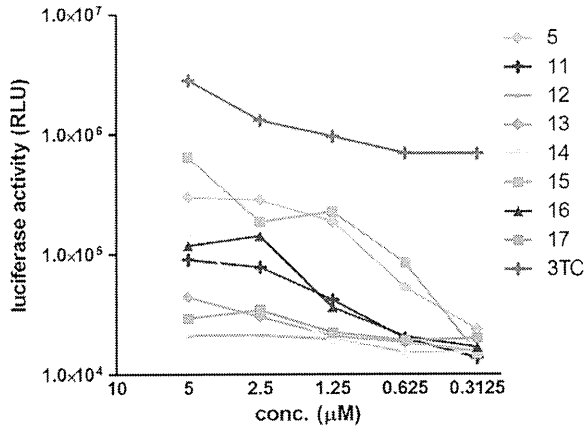

Figure 4. Luciferase signals in MT-4 Luc cells infected with HIV-1 in the presence of different concentrations of compounds **11–17**. Luciferase activity is expressed as relative luciferase units (RLU). 3TC is an HIV reverse transcriptase inhibitor, which was used as a positive control.

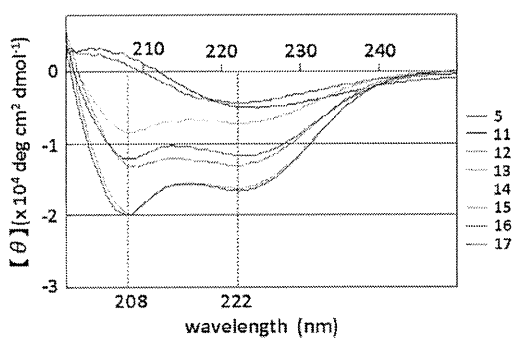

Figure 5. CD spectra of compounds **5** and **11–17** (5 μM) in 0.1 M phosphate buffer, pH 5.6 containing 50% MeOH at 25 °C.

compound **5**. Replacement of His^{14}-Gly^{18} and Ile^{3}-Leu^{7} by Glu-Lys in compounds **11** and **15**, respectively, caused a significant decrease in α-helicity, possibly due to formation of unfavorable salt bridges such as Glu^{14}-Arg^{16} and Glu^{3}-Arg^{5}. Introduction of a Glu-Lys pair into Gln^{9}-Ile^{13} in compound **13** caused a slight decrease in α-helicity, possibly due to interference in the formation of a salt bridge of Glu^{1}-Arg^{5} by that of Arg^{5}-Glu^{9}. In the other analogs, increases in α-helicity were observed to result from the introduction of Glu-Lys pairs as we had initially postulated. Overall, there is no positive correlation between IN inhibitory or anti-HIV activity and the degree of α-helicity of the compounds.

In order to identify the amino acid residues responsible for IN inhibitory and anti-HIV activities of these peptides, an Ala-scan of compound **4** was performed (Fig. 6). Compounds **18–22**, **25**, **27** and **29** showed IN inhibitory activities against the 3′-end processing and strand transfer reactions similar to those of **4** (Table 3). Ala-substitution for Leu^{7}, Gln^{8}, Gln^{9}, Leu^{10}, Leu^{11}, His^{14}, Arg^{16} or Gly^{18} did not cause any significant change in either of IN inhibitory activities, indicating that the replaced amino acids are not essential for IN inhibition. Ala-substitution for Phe^{12}, Ile^{13}, Phe^{15} or Ile^{17} gave compounds **23**, **24**, **26** and **28**, which were 2–4 times less active in both the IN inhibitory assays, suggesting that Phe^{12}, Ile^{13}, Phe^{15} and Ile^{17} are indispensable for IN inhibition. Assessment of anti-HIV activity in the MT-4 Luc system showed that all compounds **18–29** produced dose-dependent inhibition of HIV-1 replication, although they displayed cytotoxicity at 10 μM (**4**, **19–23**, **26** and **27**) or above 5 μM (**24** and **25**) (Fig. 7). Compounds **23** and **24**,

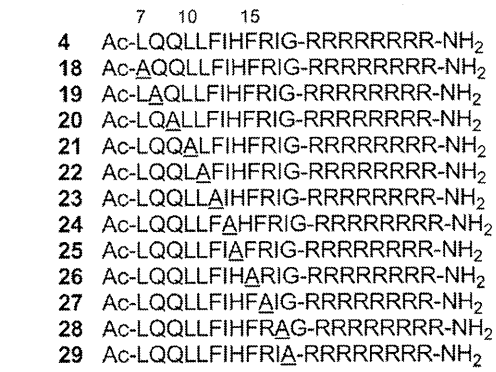

Figure 6. Amino acid sequences of compounds **18–29** based on an Ala-scan of compound **4**. Position numbers correspond to alignment with compound **5**.

Table 3
IC_{50} values of compounds **18–29** toward the 3′-end processing and strand transfer reactions catalyzed by HIV-1 IN

Compound	IC_{50} (μM)	
	3′-End processing	Strand transfer
4	0.11 ± 0.03	0.05 ± 0.01
18	0.12 ± 0.004	0.08 ± 0.01
19	0.13 ± 0.02	0.06 ± 0.01
20	0.10 ± 0.004	0.06 ± 0.01
21	0.12 ± 0.02	0.07 ± 0.01
22	0.13 ± 0.003	0.06 ± 0.01
23	0.34 ± 0.06	0.18 ± 0.03
24	0.33 ± 0.02	0.22 ± 0.01
25	0.13 ± 0.01	0.06 ± 0.01
26	0.25 ± 0.02	0.12 ± 0.01
27	0.11 ± 0.01	0.05 ± 0.01
28	0.20 ± 0.03	0.16 ± 0.02
29	0.09 ± 0.01	0.09 ± 0.01

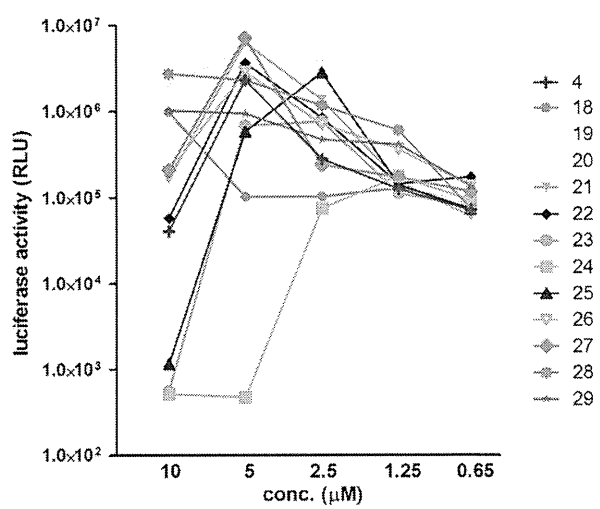

Figure 7. Luciferase signals in MT-4 Luc cells infected with HIV-1 in the presence of various concentrations of compounds **18–29**. Luciferase activity was valued as RLU.

with Ala-substitution for Phe^{12} and Ile^{13}, respectively, showed weaker inhibitory activity than **4** at 5 μM. Consequently, Phe^{12} and Ile^{13} were deemed to be critical for activity, which is consistent with the IN inhibitory activity results. A control peptide isomer of **5** (Ac-QIFEHLAGIIQILRFLRI-R_8-NH_2) did not show anti-HIV activity at

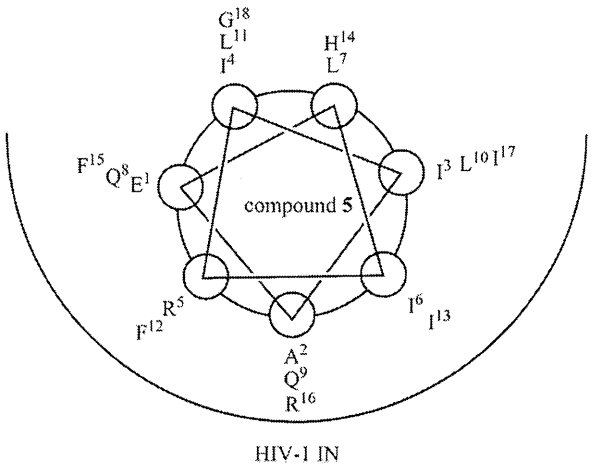

Figure 8. Brief presumed drawing of the binding model of HIV-1 IN and compound **5**.

concentrations below 10 μM, suggesting that the original Vpr-sequence, with the exceptions of Phe^{12}, Ile^{13}, Phe^{15} and Ile^{17}, is critical for activity.

The assumption that compound **5** forms an α-helical structure when binding to HIV-1 IN suggests the binding model of IN and **5** shown in Figure 8, as **5** forms an α-helical structure in 50% aqueous MeOH solution. In this model, Phe^{12}, Ile^{13}, Phe^{15} and Ile^{17}, which were identified by the Ala-scan experiment as critical residues, are located in the pocket of IN. His^{14} and Gly^{18}, which can be replaced by Glu-Lys with an increase of activity in compound **11**, are located outside of the pocket of IN. Ile^{3} and Leu^{7} can also be replaced by Glu-Lys while retaining activity in compound **15**, and Leu^{7} is located outside of the pocket, whereas Ile^{3} is located in the edge of the pocket. Compounds **11** and **15** might form α-helical structures when binding to IN, although **11** or **15** does not show α-helicity in the CD spectrum. Thus, these compounds might retain IN inhibitory activity. This binding model is compatible with the results of structure–activity relationship studies involving Glu-Lys substitution and Ala-scan. The reason for decreases in IN inhibitory and anti-HIV activity of compounds **12** and **17**, which show increases of α-helicity, are possibly due to substitution of Glu-Lys for Ala^{2} and Ile^{6}, which are located in the pocket of IN. The reason for a decrease in activity of compounds **14** and **16**, which show increased α-helicity, might be due to substitution of Lys for Gln^{8} and Phe^{15}, respectively, which are located in the pocket of IN. The reason for decreases in IN inhibitory and anti-HIV activity of compound **13**, which also shows a decrease of α-helicity, are possibly due to substitution of Glu-Lys for Gln^{9} and Ile^{13}, which are located in the pocket of IN.

3. Conclusion

In the present study, structure–activity relationship studies were performed on Vpr-derived peptides **4** and **5**, which had been previously identified as HIV-1 IN inhibitors.[4] The Glu-Lys substitution experiments and Ala-scan data suggest that several amino acid residues of **4** and **5** are indispensable for IN inhibitory and anti-HIV activities, and a binding model of IN and **5** were proposed. Furthermore, two novel compounds **11** and **15**, which contained Glu-Lys pairs and showed more potent IN inhibitory activities than compound **5**, were found. These data including the binding model should be useful for the development of potent HIV-1 IN inhibitors based on Vpr-peptides.

4. Experimental

4.1. Chemistry

All peptides were synthesized by the Fmoc-based solid-phase method. The synthetic peptides were purified by RP-HPLC and identified by ESI-TOF-MS. Fmoc-protected amino acids and reagents for peptide synthesis were purchased from Novabiochem, Kokusan Chemical Co., Ltd and Watanabe Chemical Industries, Ltd. Protected peptide resins were constructed on NovaSyn TGR resins (0.26 meq/g, 0.025 and 0.0125 mmol scales for Glu-Lys substitution and Ala-scan peptides, respectively). All peptides were synthesized by stepwise elongation techniques. Each cycle involves (i) deprotection of an Fmoc group with 20% (v/v) piperidine/DMF (10 mL) for 15 min and (ii) coupling with 5.0 equiv of Fmoc-protected amino acid, 5.0 equiv of diiopropylcarbodiimide (DIPCI) and 5.0 equiv of 1-hydroxybenzotriazole monohydrate ($HOBt{\cdot}H_2O$) in DMF (3 mL) for 90 min. N-Terminal α-amino groups of Glu-Lys substitution and Ala-scan peptides were acetylated with 100 equiv of acetic anhydride in DMF (10 mL). Cleavage from the resin and side chain deprotection were carried out by stirring for 1.5 h with *m*-cresol (0.25 mL), thioanisole (0.75 mL), 1,2-ethanedithiol (0.75 mL) and TFA (8.25 mL). After removal of the resins by filtration, the filtrate was concentrated under reduced pressure, the crude peptides were precipitated in cooled diethyl ether and purified by preparative RP-HPLC on a Cosmosil 5C18-AR II column (10 × 250 mm, Nacalai Tesque, Inc.) with a LaChrom Elite HTA system (Hitachi). The HPLC solvents employed were water containing 0.1% TFA (solvent A) and acetonitrile containing 0.1% TFA (solvent B). All peptides were purified using a linear gradient of solvents A and B over 30 min at a flow rate of 3 $cm^3\ min^{-1}$. The purified peptides were identified by ESI-TOF-MS (Brucker Daltonics micrOTOF-2focus) (shown in Table S1 in Supplementary data). All peptides were obtained after lyophilization as fluffy white powders of the TFA salts. The purities of these peptides were checked by analytical HPLC on a Cosmosil 5C18-ARII column (4.6 × 250 mm, Nacalai Tesque, Inc.) eluted with a linear gradient of solvents A and B at a flow rate of 1 $cm^3\ min^{-1}$, and eluted products were detected by UV at 220 nm (shown in Figs. S1–S3 in Supplementary data).

4.2. Expression and purification of F185K/C280S HIV-1 integrase from *Escherichia coli*

Plasmid encoding IN1–288/F185K/C280S was expressed in *Escherichia coli* strain C41. The solubility of the mutant protein was examined in a crude cell lysate, as follows. Cells were grown in 1 L of culture medium containing 100 μg/mL of ampicillin at 37 °C until the optical density of the culture at 600 nm was between 0.4 and 0.9. Protein expression was induced by the addition of isopropyl-1-thio-β-D-galactopyranoside to a final concentration of 0.1 mM. After 2 h, the cells were collected by centrifugation at 6000 rpm for 30 min. After removal of the supernatant, the cells were resuspended in HED buffer (20 mM HEPES, pH 7.5, 1 mM EDTA, 1 mM DTT) with 0.5 mg/mL lysozyme and stored on ice for 30 min. The cells were sonicated until the solution exhibited minimal viscosity then it was centrifuged at 15,000 rpm for 30 min. After removal of the supernatant, the pellet was dissolved in TNM buffer (20 mM Tris/HCl, pH 8.0, 1 M NaCl, 2 mM 2-mercaptoethanol) with 5 mM imidazole and stored on ice for 30 min. The cells were then centrifuged at 15,000 rpm for 30 min and the supernatant was collected. The supernatant was then filtered through 0.45 μm filter cartridge and applied to a HisTrap column at 1 mL/min flow rate. After loading, the column was washed with 10 volume of TNM buffer with 5 mM imidazole. Protein was eluted with a linear gradient of 500 mM imidazole, containing TNM buf-

fer. Fractions containing IN were pooled and checked with SDS–PAGE.

4.3. CD spectroscopy of peptides with Glu-Lys substitution

CD measurements were performed on a JASCO J720 spectropolarimeter equipped with thermo-regulator (JASCO Corp., Ltd), using 5 μM of peptides dissolved in 0.1 M phosphate buffer, pH 5.6 containing 50% MeOH. UV spectra were recorded at 25 °C in a quartz cell 1.0 mm path length, a time constant of 1 s, and a 100 nm/min scanning speed with 0.1 nm resolution.

4.4. Integrase assays

Expression and purification of the recombinant IN in *E. coli* were performed as previously reported with addition of 10% glycerol to all buffers. Oigonucleotide substrates were prepared as described.[6] Integrase reactions were performed in 10 μL with 400 nM of recombinant IN, 20 nM of 5′-end [^{32}P]-labeled oligonucleotide substrate and inhibitors at various concentrations. Solutions of 10% DMSO without inhibitors were used as controls. Reaction mixtures were incubated at 37 °C (60 min) in buffer containing 50 mM MOPS, pH 7.2, 7.5 mM $MgCl_2$, and 14.3 mM 2-mercaptoethanol. Reactions were stopped by addition of 10 μL of loading dye (10 mM EDTA, 98% deionized formamide, 0.025% xylene cyanol and 0.025% bromophenol blue). Reactions were then subjected to electrophoresis in 20% polyacrylamide–7 M urea gels. Gels were dried and reaction products were visualized and quantitated with a Typhoon 8600 (GE Healthcare, Little Chalfont, Buckinghamshire, UK). Densitometric analyses were performed using ImageQuant from Molecular Dynamics Inc. The concentrations at which enzyme activity was reduced by 50% (IC_{50}) were determined using 'Prism' software (GraphPad Software, San Diego, CA) for nonlinear regression to fit dose–response data to logistic curve models.

4.5. Replication assays (MT-4 luciferase assays)

MT-4 luciferase cells (1×10^3 cells) grown in 96-well plates were infected with HIV-1_{HXB2} in the presence of various concentrations of peptides. At 6–7 days post-infection, cells were lysed and the luciferase activities were measured using the Steady-Glo assay kit (Promega), according to the manufacturer's protocol. Chemiluminescence was detected with a Veritas luminometer (Promega).

Acknowledgments

N.O. and T.T. are supported by JSPS research fellowships for young scientists. This work was supported by Mitsui Life Social Welfare Foundation, Grant-in-Aid for Scientific Research from the Ministry of Education, Culture, Sports, Science, and Technology of Japan, the Health and Labour Sciences Research Grants from Japanese Ministry of Health, Labor, and Welfare, and by the NIH Intramural Program, Center for Cancer Research, US National Cancer Institute.

Supplementary data

Supplementary data associated with this article can be found, in the online version, at doi:10.1016/j.bmc.2010.07.050.

References and notes

1. Mitsuya, H.; Erickson, J. In *Textbook of AIDS Medicine*; Merigan, T C., Bartlett, J. G., Bolognesi, D., Eds.; Williams & Wilkins: Baltimore, 1999; pp 751–780.
2. (a) Cahn, P.; Sued, O. *Lancet* **2007**, *369*, 1235; (b) Grinsztejn, B.; Nguyen, B.-Y.; Katlama, C.; Gatell, J. M.; Lazzarin, A.; Vittecoq, D.; Gonzalez, C. J.; Chen, J.; Harvey, C. M.; Isaacs, R. D. *Lancet* **2007**, *369*, 1261.
3. (a) Farnet, C. M.; Bushman, F. D. *Cell* **1997**, *88*, 483; (b) Chen, H.; Engelman, A. *Proc. Natl. Acad. Sci. U.S.A.* **1998**, *95*, 15270; (c) Gleenberg, I. O.; Herschhorn, A.; Hizi, A. *J. Mol. Biol.* **2007**, *369*, 1230; (d) Gleenberg, I. O.; Avidan, O.; Goldgur, Y.; Herschhorn, A.; Hizi, A. *J. Biol. Chem.* **2005**, *280*, 21987; (e) Hehl, E. A.; Joshi, P.; Kalpana, G. V.; Prasad, V. R. *J. Virol.* **2004**, *78*, 5056; (f) Tasara, T.; Maga, G.; Hottiger, M. O.; Hubscher, U. *FEBS Lett.* **2001**, *507*, 39; (g) Gleenberg, I. O.; Herschhorn, A.; Goldgur, Y.; Hizi, A. *Arch. Biochem. Biophys.* **2007**, *458*, 202.
4. Suzuki, S.; Urano, E.; Hashimoto, C.; Tsutsumi, H.; Nakahara, T.; Tanaka, T.; Nakanishi, Y.; Maddali, K.; Han, Y.; Hamatake, M.; Miyauchi, K.; Pommier, Y.; Beutler, J. A.; Sugiura, W.; Fuji, H.; Hoshino, T.; Itotani, K.; Nomura, W.; Narumi, T.; Yamamoto, N.; Komano, J. A.; Tamamura, H. *J. Med. Chem.* **2010**, *53*, 5356.
5. Suzuki, T.; Futaki, S.; Niwa, M.; Tanaka, S.; Ueda, K.; Sugiura, Y. *J. Biol. Chem.* **2002**, *277*, 2437.
6. (a) Yan, H.; Mizutani, T. C.; Nomura, N.; Tanaka, T.; Kitamura, Y.; Miura, H.; Nishizawa, M.; Tatsumi, M.; Yamamoto, N.; Sugiura, W. *Antivir. Chem. Chemother.* **2005**, *16*, 363; (b) Marchand, C.; Zhang, X.; Pais, G. C. G.; Cowansage, K.; Neamati, N.; Burke, T. R., Jr.; Pommier, Y. *J. Biol. Chem.* **2002**, *277*, 12596; (c) Semenova, E. A.; Johnson, A. A.; Marchand, C.; Davis, D. A.; Tarchoan, R.; Pommier, Y. *Mol. Pharmacol* **2006**, *69*, 1454; (d) Leh, H.; Brodin, P.; Bischerour, J.; Deprez, E.; Tauc, P.; Brochon, J. C.; LeCam, E.; Coulaud, D.; Auclair, C.; Mouscadet, J. F. *Biochemistry* **2000**, *39*, 9285; (e) Marchand, C.; Neamati, N.; Pommier, Y. In Vitro Human Immunodeficiency Virus Type 1 Integrase Assays. In *Methods in Enzymology (Drug-Nucleic Acid Interactions)*; Chaires, J. B., Waring, M. J., Eds.; Elsevier: Amsterdam, 2001; Vol. 340, pp 624–633.
7. Morellet, N.; Bouaziz, S.; Petitjean, P.; Roques, B. P. *J. Mol. Biol.* **2003**, *327*, 215.

5356 *J. Med. Chem.* **2010,** *53,* 5356–5360
DOI: 10.1021/jm1003528

Journal of
Medicinal
Chemistry
Brief Article

Peptide HIV-1 Integrase Inhibitors from HIV-1 Gene Products

Shintaro Suzuki,[†,#] Emiko Urano,[‡,#] Chie Hashimoto,[†] Hiroshi Tsutsumi,[†] Toru Nakahara,[†] Tomohiro Tanaka,[†] Yuta Nakanishi,[†] Kasthuraiah Maddali,[§] Yan Han,[‡] Makiko Hamatake,[‡] Kosuke Miyauchi,[‡] Yves Pommier,[§] John A. Beutler,[⊥] Wataru Sugiura,[‡] Hideyoshi Fuji,[∥] Tyuji Hoshino,[∥] Kyoko Itotani,[†] Wataru Nomura,[†] Tetsuo Narumi,[†] Naoki Yamamoto,[‡] Jun A. Komano,[‡] and Hirokazu Tamamura*[,†]

[†]*Department of Medicinal Chemistry, Institute of Biomaterials and Bioengineering, Tokyo Medical and Dental University, 2-3-10 Kandasurugadai, Chiyoda-ku, Tokyo 101-0062, Japan,* [‡]*AIDS Research Center, National Institute of Infectious Diseases, 1-23-1 Toyama, Shinjuku-ku, Tokyo 162-8640, Japan,* [§]*Laboratory of Molecular Pharmacology, Center for Cancer Research, National Cancer Institute, National Institutes of Health, Bethesda, Maryland 20892-4255,* [∥]*Department of Physical Chemistry, Graduate School of Pharmaceutical Sciences, Chiba University, 1-33 Yayoi-cho, Inage-ku, Chiba 263-8522, Japan, and* [⊥]*Molecular Targets Laboratory, Center for Cancer Research, National Cancer Institute, National Institutes of Health, Frederick, Maryland 21702.* [#] *These authors contributed equally to this work.*

Received March 17, 2010

Anti-HIV peptides with inhibitory activity against HIV-1 integrase (IN) have been found in overlapping peptide libraries derived from HIV-1 gene products. In a strand transfer assay using IN, inhibitory active peptides with certain sequential motifs related to Vpr- and Env-derived peptides were found. The addition of an octa-arginyl group to the inhibitory peptides caused a remarkable inhibition of the strand transfer and 3′-end-processing reactions catalyzed by IN and significant inhibition against HIV replication.

Introduction

Many antiretroviral drugs are currently available to treat human immunodeficiency virus type 1 (HIV-1) infection. Viral enzymes such as reverse transcriptase (RT[a]), protease and integrase (IN), gp41, and coreceptors are the main targets for antiretroviral drugs that are under development. Because of the emergence of viral strains with multidrug resistance (MDR), however, new anti-HIV-1 drugs operating with different inhibitory mechanisms are required. Following the success of raltegravir, IN has emerged as a prime target. IN is an essential enzyme for the stable infection of host cells because it catalyzes the insertion of viral DNA inside the preintegration complex (PIC) into the genome of host cells in two successive reactions, designated as strand transfer and 3′-end-processing. It is assumed that the enzymatic activities of IN have to be negatively regulated in the PIC during its transfer from the cytoplasm to the nucleus. Otherwise, premature activation of IN can lead to the autointegration into the viral DNA itself, resulting in an aborted infection. We speculate that the virus, rather than the host cells, must encode a mechanism to prevent autointegration. The PIC contains in association with the viral nucleic acid, viral proteins such as RT, IN, capsids ($p24^{CA}$ and $p7^{NC}$), matrix ($p17^{MA}$), p6 and Vpr, cellular proteins HMG I (Y), and the barrier to autointegration factor (BAF).[1−4] It is likely that, due to their spatial proximity in the PIC, these proteins physically and functionally interact with each other. For instance, it is already known that RT activity inhibited by Vpr,[5] and that RT and IN inhibit each other.[5−9] Vpr also inhibits IN through its C-terminal domain.[5,10] Because these studies suggest that PIC components regulate each other's function, we have attempted to obtain potent inhibitory lead compounds from a peptide fragment library derived from HIV-1 gene products, an approach which has been successful in finding a peptide IN inhibitor from LEDGF, a cellular IN binding protein.[11]

In this paper, we describe the screening of an overlapping peptide library derived from HIV-1 proteins, the identification of certain peptide motifs with inhibitory activity against HIV-1 IN, and the evaluation of effective inhibition of HIV-1 replication in cells using the identified peptide inhibitors possessing cell membrane permeability.

Results and Discussion

An overlapping peptide library spanning HIV-1 SF2 *Gag*, *Pol*, *Vpr*, *Tat*, *Rev*, *Vpu*, *Env*, and *Nef*, provided by Dr. Iwamoto of the Institute of Medical Science at the University of Tokyo (Supporting Information, SI, Figure 2A), was screened with a strand transfer assay[12] in search of peptide pools with inhibitory activity against HIV-1 IN. The library consists of 658 peptide fragments derived from the HIV-1 gene products. Each peptide is composed of 10−17 amino acid residues with overlapping regions of 1−7 amino acid residues. Sixteen peptide pools containing between 16 and 65 peptides were used for the first screening at the final concentration of 5.0 μM for each peptide (SI Figure 2B). This initial screening gave the results shown in Figure 1. Both Vpr and Env4 pools showed remarkable inhibition of IN strand transfer activity, and consequently a second screening was performed using the individual peptides contained in the Vpr and Env4 pools. A group of consecutive overlapping peptides in the Vpr pool (groups 13−15) and groups 4−6 and 20−21 in the Env4 pool were found to possess IN inhibitory activity (Figure 2). We focused on Vpr15 and Env4-4 peptides because they showed inhibitory activity against IN strand transfer reaction in a dose-dependent manner (Figure 3). The IC_{50} values of Vpr15

*To whom correspondence should be addressed. Phone: +81-3-5280-8036. Fax: +81-3-5280-8039. E-mail: tamamura.mr@tmd.ac.jp.

[a]Abbreviations: HIV, human immunodeficiency virus; IN, integrase; RT, reverse transcriptase; MDR, multidrug resistance; PIC, preintegration complex; BAF, barrier to autointegration factor; R_8, octa-arginyl.

 Published on Web 06/29/2010

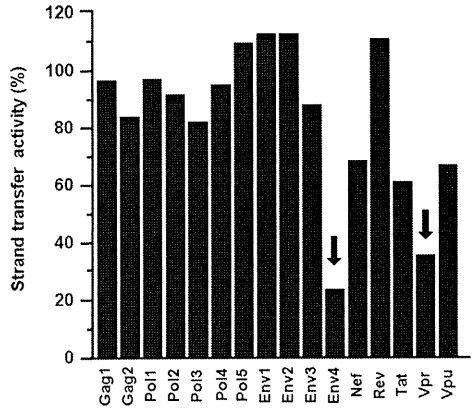

Figure 1. Inhibition of the IN strand transfer activity by peptide pools. Inhibition of the IN strand transfer activity was strongly inhibited by Env4 and Vpr pools (arrows). The *y*-axis represents the IN strand transfer activity relative to the solvent control (DMSO).

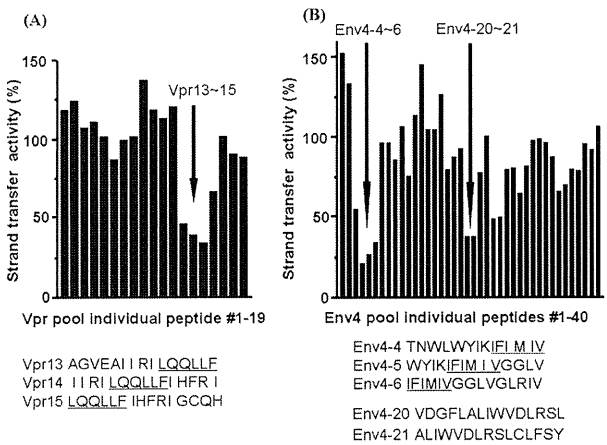

Figure 2. Identification of IN inhibitory peptides in the Vpr (A) and Env4 (B) pools based on the strand transfer activity of IN. The consecutive overlapping peptides display the inhibition of the strand transfer activity of IN (arrows). The *y*-axis represents the IN strand transfer activity relative to the solvent control (DMSO). The concentration of each peptide was 5 μM. The common sequences of individual peptides derived from Vpr and Env4 pools with anti-IN activity are underlined.

and Env4-4 were estimated at 5.5 and 1.9 μM, respectively. These peptides did not show any significant inhibitory activity against HIV-1 RT, suggesting that they might inhibit IN strand transfer reaction selectively.

The overlapping peptides of Vpr13-15 and Env4-4-6 have the vommon hexapeptide sequences LQQLLF and IFIMIV, respectively. The LQQLLF sequence covers positions 64−69 of Vpr, which is a part of the second helix of Vpr. The IFIMIV sequence corresponds to positions 684−689 of gp160, which is a part of the transmembrane domain of TM/gp41. These hexapeptides are thought to be critical to inhibition of IN activity. It was recently reported[5] that similar peptides derived from Vpr inhibit IN with IC_{50} values of 1−16 μM, which is consistent with our data. In this report,[5] the peptide motif was found to be 15 amino acid residues spanning LQQLLF from the overlapping Vpr peptide library. In our study, more precise mapping of inhibitory motif in Vpr peptides was achieved by identifying the shorter effective peptide motif. We focused on the Vpr-derived peptide, LQQLLF (Vpr-1) to develop potent inhibitory peptides. However, the expression of inhibitory activity against IN

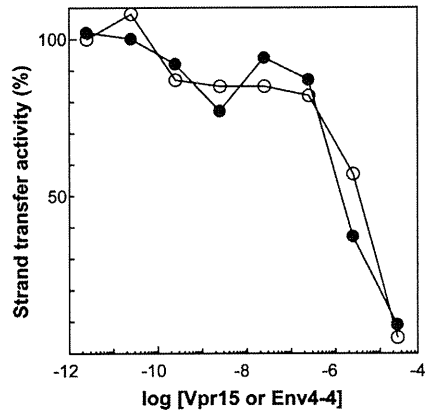

Figure 3. Concentration-dependent inhibition of IN strand transfer activities by Vpr15 (○) and Env4−4 (●) peptides. The *y*-axis represents the IN strand transfer activity relative to the solvent control (DMSO).

in vivo by only hexapeptides might be difficult because these hexapeptides penetrate the plasma membrane very poorly and to achieve antiviral activity, it is essential that they penetrate the cell membrane. To that effect, an octa-arginyl (R_8) group[13] was fused to the Vpr-derived peptides (Table 1). R_8 is a cell membrane permeable motif and its fusion with parent peptides successfully generates bioactive peptides without significant adverse effects or cytotoxicity.[14−18] In addition, the R_8-fusion could increase the solubility of Vpr-derived peptides which have a relatively hydrophobic character.

The inhibitory activity of Vpr-1 and Vpr-1-4 R_8 peptides against IN was evaluated based on the strand transfer and 3′-end-processing reactions in vitro (Table 1).[19,20] Vpr-1 did not show strong inhibition of either IN activity, but the IC_{50} of Vpr-1 R_8 toward the strand transfer reaction of IN was 10-fold lower than that of Vpr-1 lacking the R_8 group. This indicates that the positive charges derived from the R_8 group might enhance the inhibitory activity of the Vpr-1 peptide. Because we were concerned that the strong positive charges close to the LQQLLF motif might interfere with the inhibitory activity, the 6 amino acid sequence (−IHFRIG−) was inserted as a spacer between LQQLLF and R_8 (Vpr-3 R_8). The IHFRIG sequence was used to reconstitute the natural Vpr. The IC_{50} values of Vpr-2 R_8 for the strand transfer and 3′-end-processing activities of IN were 0.70 and 0.83 μM, respectively, while Vpr-3 R_8 showed potent IN inhibitory activities of 4.0 and 8.0 nM against the strand transfer and 3′-end- processing activities, respectively. This result indicates the additional importance of the IHFRIG sequence for inhibitory activities against IN. The increased IN inhibitory activities might be achieved presumably by the synergistic effect of the LQQLLF motif, the IHFRIG sequence, and the R_8 group. Vpr-4 R_8, in which the EAIIRI sequence was attached to further reconstitute the Vpr helix 2, showed inhibitory activities similar to those of Vpr-3 R_8, suggesting that reconstitution of helix 2 of Vpr is not necessary for efficient IN inhibition. Vpr-3 R_8 and Vpr-4 R_8, with $IC_{50} > 0.5\,\mu$M,[21] were less potent inhibitors of RT-associated RNase H activity, indicating that these peptides can selectively inhibit IN. These results suggest that Vpr-derived peptides are novel and distinct from any other IN inhibitors reported to date.

For rapid assessment of the antiviral effect of Vpr-derived peptides, we established an MT-4 Luc system in which MT-4 cells were stably transduced with the firefly luciferase expression cassette by a murine leukemia viral vector (SI Figure 3).

Table 1. Sequences of Vpr-Derived Peptides and Their IC_{50} Values toward the Strand Transfer and 3′-End Processing Reactions of IN

	sequence	IC_{50} (μM)	
		strand transfer	3′-end processing
Vpr-1	LQQLLF	68 ± 1.0	> 100
Vpr-1 R_8	Ac-LQQLLF -R_8-NH_2	6.1 ± 1.1	> 11
Vpr-2 R_8	Ac-IHFRIG-R_8-NH_2	0.70 ± 0.06	0.83 ± 0.07
Vpr-3 R_8	Ac-LQQLLF IHFRIG-R_8-NH_2	0.004 ± 0.0001	0.008 ± 0.001
Vpr-4 R_8	Ac-EAIIRI LQQLLF IHFRIG-R_8-NH_2	0.005 ± 0.002	0.006 ± 0.006

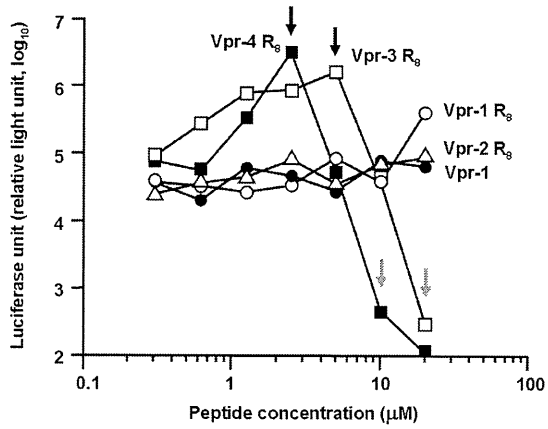

Figure 4. Luciferase signals in MT-4 Luc cells infected with HIV-1 in the presence of various concentrations of Vpr-derived peptides: Vpr-1 (●), Vpr-1 R_8 (○), Vpr-2 R_8 (△), Vpr-3 R_8 (□), Vpr-4 R_8 (■).

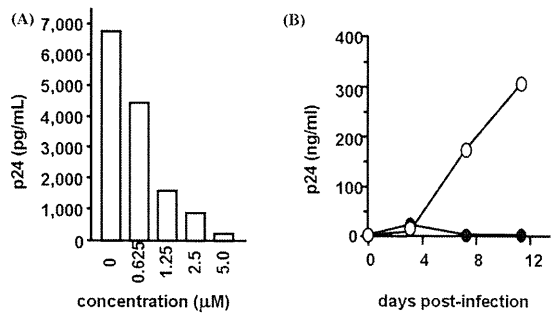

Figure 5. (A) The inhibition of HIV-1_{JR-CSF} replication in NP2-CD4-CCR5 cells in the presence of various concentrations of Vpr-3 R_8. (B) The replication kinetics of HIV-1_{HXB2} in MT-4 cells in the presence of Vpr-3 R_8 (●). The concentration of Vpr-3 R_8 was fixed at 0.5 μM. Absence of Vpr-3 R_8 (○).

MT-4 Luc cells constitutively express high levels of luciferase which are significantly reduced by HIV-1 infection due to their high susceptibility to cell death upon HIV-1 infection. Protection of MT-4 Luc cells from HIV-1-induced cell death maintains the luciferase signals at high levels. In addition, the cytotoxicity of Vpr-derived peptides can be evaluated by a decrease of luciferase signals in these MT-4 Luc systems. Vpr-2 R_8, which is a weak IN inhibitor, showed no significant anti-HIV-1 activity below concentrations of 20 μM, suggesting that its moderate IC_{50} level in vitro is not sufficient to suppress HIV-1 replication in tissue culture and that the R_8 group is not significantly cytotoxic (Figure 4). Vpr-1 did not show any inhibitory effects against HIV-1 replication; however, Vpr-1 R_8 displayed a weak antiviral effect at a concentration of 20 μM and both Vpr-3 R_8 and Vpr-4 R_8 showed significant inhibitory effects against HIV-1 replication. The R_8 peptide did not show significant anti-HIV activity (IC_{50} > 50 μM, data not shown). These results suggest that the addition of the R_8 group enables Vpr-derived peptides to enter the cytoplasm and access IN, with the result that HIV-1 replication could be effectively inhibited.

Because Vpr-3 R_8 was less cytotoxic than Vpr-4 R_8, the inhibitory activities of Vpr-3 R_8 were further investigated. Two replication assay systems, R5-tropic HIV-1_{JR-CSF} on NP2-CD4-CCR5 cells and X4-tropic HIV-1_{HXB2} on MT-4 cells, were utilized. NP2-CD4-CCR5 cells were infected with HIV-1_{JR-CSF} in the presence of various concentrations of Vpr-3 R_8. On day 4 postinfection, the culture supernatant was collected and the concentration of viral p24 antigen was measured by an ELISA assay. The p24 levels decreased in a dose-dependent manner with increasing the concentration of Vpr-3 R_8; 50% inhibition of p24 expression was obtained with approximately 0.8 μM of Vpr-3 R_8 (Figure 5A). This concentration was approximately 10-fold lower than the concentration of Vpr-3 R_8 known to be cytotoxic (Figure 4). Second, MT-4 cells were infected with HIV-1_{HXB2} and the replication kinetics was monitored in the presence of 0.5 μM Vpr-3 R_8. The degree of replication of HIV-1_{HXB2} was quite low in the presence of Vpr-3 R_8, while replication of HIV-1_{HXB2} was robust in the absence of Vpr-3 R_8 (Figure 5B), suggesting that Vpr-3 R_8 strongly suppresses the replication of HIV-1 in cells. To examine whether the HIV-1 replication was blocked through the inhibition of IN activity, quantitative real-time PCR was performed. If IN is inhibited, the efficiency of viral genome integration should be decreased while the reverse transcription of viral genome should not be affected. Accordingly, NP2-CD4-CXCR4 cells were infected with HIV-1_{HXB2} in the presence or absence of 0.5 μM Vpr-3 R_8. Genomic DNA was extracted on day 2 postinfection, and the viral DNA was quantified at the various steps of viral entry phase. The level of "strong stop DNA", representing the total genome of infected virus in Vpr-3 R_8-treated cells, was similar (139.7%) to that in DMSO-treated control cells and the level of viral DNA generated at the late stage of reverse transcription in Vpr-3 R_8-treated cells was slightly decreased (84.4%) compared to control cells. This small decline can probably be attributed to the weak anti-RNase H activity of Vpr-3 R_8. On the other hand, a drastic decrease of Alu-LTR products was observed in Vpr-3 R_8-treated cells (15.8%), indicating an inhibition of integrated viral genome. Concomitantly, the double LTR products, representing the end-joined viral genome catalyzed by host cellular enzymes, were increased by a factor of 8 (779.8%). These results strongly suggest that Vpr-3 R_8 blocks viral infection by inhibiting IN activity in cells, consistent with our in vitro observations. Judging by these results, Vpr-derived peptides with the R_8 group are potent IN inhibitors that suppress HIV-1 replication in vivo.

Finally, in silico molecular docking simulations of Vpr-derived peptides and HIV-1 IN were performed. The Vpr-derived peptides are located in the second helix of Vpr and were thus considered to have an α-helical conformation.[22] Docking simulations of three peptides (Vpr13, Vpr14, and Vpr15), using the predicted structure of the HIV-1 IN dimer as a template,[23] were performed by GOLD software to investigate the binding mode of the peptides, the binding affinity of

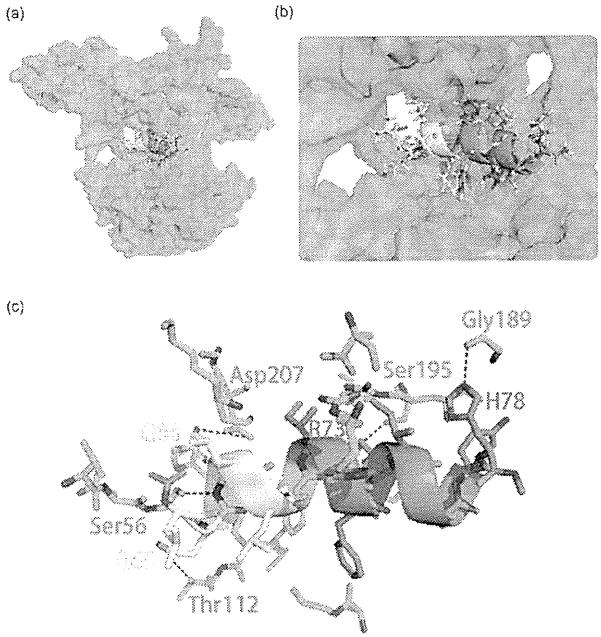

Figure 6. Predicted binding mode of Vpr15 to HIV-1 IN by GOLD. An overall view of (a) the complex obtained by docking Vpr15 with the HIV-1 IN dimer and (b) the closer view of the complex. The predicted structure of full-length HIV-1 IN was used as a template. Each HIV-1 IN monomer was shown as green or cyan surface. The docked Vpr15 is shown as a cartoon. The yellow-colored region is the LQQLLF motif. The GOLD score representing the docking complementarity is 69.83, indicating the high binding affinity between Vpr15 and IN. The hydrogen-bond interactions between HIV-1 IN and Vpr15 were presented by LIGPLOT software shown as blue dotted line (c).

the peptides being evaluated by GOLD Fitness score. The predicted binding mode of Vpr15 to IN is shown in Figure 6. Our results predict that the three Vpr-derived peptides interact with the cleft between the amino-terminal domain and the core domain of HIV-1 IN. This region is distinct from the nucleic acid interacting surfaces, indicating that the Vpr-derived peptides inhibit IN function in an allosteric manner. A previous report provided a model in which a Vpr peptide was bound to IN in a manner similar with our model[5] and, interestingly, the peptides were bound to IN with an exterior surface of Vpr. This earlier report that the full-length Vpr inhibits IN[10] strongly supports the predicted binding mode of Vpr15. Five hydrogen-bond interactions between HIV-1 IN and Vpr15 were identified by LIGPLOT analysis,[24] which invoked the following IN-Vpr amino acids: IN Thr112-Vpr Gln65, IN Ser56-Vpr Gln66, IN Asp207-Vpr Gln66, IN Ser195-Vpr Arg73, and IN Gly189-Vpr His78. The numbering of Vpr amino acids is based on the Vpr full-length coordinate, Figure 6. Additional hydrophobic contacts between IN and Vpr15 were found in which the following IN-Vpr amino acid pairs are involved: IN Lys211-Vpr Gln66, IN Pro109-Vpr Phe69, IN Arg262-Vpr His71, and IN Arg187-Vpr Gln77. These data indicate that the Gln65, Gln66, and Phe69 residues in Vpr-derived peptides play a major role in the interaction between IN and Vpr-derived peptides.

Conclusions

In summary, two peptide motifs, LQQLLF from Vpr and IFIMIV from Env4, possessing inhibitory activity against HIV-1 IN, were identified through the screening of overlapping peptide library derived from HIV-1 gene products. We initially speculate that HIV encodes a mechanism to prevent autointegration in the PIC because integration activity must be regulated until the virus infects cells. This speculation is supported by the finding that IN inhibitors exist in the viral PIC components. Vpr-derived peptides with the R_8 group showed remarkable inhibitory activities against the strand transfer and 3′-end-processing reactions catalyzed by HIV-1 IN in vitro. In addition, Vpr-3 R_8 and Vpr-4 R_8 were shown to inhibit HIV-1 replication with submicromolar IC_{50} values in cells using the MT-4 Luc cell system. In the quantitative analysis of p24 antigen, 50% inhibition of HIV-$1_{JR\text{-}CSF}$ replication was caused by approximately 0.8 μM of Vpr-3 R_8, and the replication of HIV-1_{HXB2} was extensively suppressed in the long term by Vpr-3 R_8 at 0.5 μM concentrations. Our finding suggest that these peptides could serve as lead compounds for novel IN inhibitors. Amino acid residues critical to the interaction of Vpr-derived peptides with IN were identified by our in silico molecular docking simulations, and suggests that more potent peptides[25] or peptidomimetic IN inhibitors represent a novel avenue for future small molecule inhibitors of IN and HIV integration.

Experimental Section

Peptide Synthesis. Vpr-derived peptides containing the R_8 group were synthesized by stepwise elongation techniques of Fmoc-protected amino acids on NovaSyn TGR resin. Coupling reactions were performed using 5.0 equiv of Fmoc-protected amino acid, 5.0 equiv of diisopropylcarbodiimide, and 5.0 equiv of 1-hydroxybenzotriazole monohydrate. Cleavage of peptides from resin and side chain deprotection were carried out with 10 mL of TFA in the presence of 0.25 mL of *m*-cresol, 0.75 mL of thioanisole, 0.75 mL of 1,2-ethanedithiol, and 0.1 mL of water as scavenger by stirring for 1.5 h. After filtration of the deprotected peptides, the filtrate was concentrated under reduced pressure, and crude peptides were precipitated in cooled diethyl-ether. All crude peptides were purified by RP-HPLC and identified by MALDI-TOFMS. Purities of all final compounds were confirmed (>95% purity) by analytical HPLC. Detailed data are provided in SI.

Enzyme Assays. The strand transfer assay for the first screening was performed as described previously.[12] The IN strand transfer and 3′-end-processing assays for peptide motif characterizations were performed as described previously.[19,20] RNase H activity was measured as described by Beutler et al.[21]

Replication Assays. For HIV-1 replication assays, 1×10^5 cells were incubated at room temperature for 30 min with an HIV-1 containing culture supernatant (ca. 0.2−50 ng p24) and then washed and incubated. Culture supernatants were collected at different time points, and then the cells were passaged if necessary. Levels of p24 antigen were measured using a Retro TEK p24 antigen ELISA kit, according to the manufacture's protocol. Signals were detected using an ELx808 microplate photometer.

For MT-4 Luc assays, MT-4 Luc cells (1×10^3 cells) grown in 96-well plates were infected with HIV-1_{XHB2} (ca. 0.2−10 ng p24) in the presence of varying concentrations of Vpr-3 R_8. At 6−7 d postinfection, cells were lysed and luciferase activity was measured using the Steady-Glo assay kits according to the manufacture's protocol. Chemiluminescence was detected with a Veritas luminometer.

Acknowledgment. We thank Prof. A. Iwamoto's group of the Institute of Medical Science at the University of Tokyo for the peptide libraries and Dr. M. Nicklaus from NCI/NIH for providing the modeled structure of full-length HIV-1 IN. T.T. is supported by JSPS research fellowships for young scientists.

This work was supported in part by Grant-in-Aid for Scientific Research from the Ministry of Education, Culture, Sports, Science, and Technology of Japan, and Health and Labor Sciences Research Grants from Japanese Ministry of Health, Labor, and Welfare. K.M. and Y.P. are supported by the Intramural Program of the National Cancer Institute, Center for Cancer Research.

Supporting Information Available: Additional experimental procedures including MS data and figures; HPLC charts of final compounds, explanation for HIV-1 genes and the peptide pools, and illustration of MT-4 Luc system. This material is available free of charge via the Internet at http://pubs.acs.org.

References

(1) Bukrinsky, M. I.; Haggerty, S.; Dempsey, M. P.; Sharova, N.; Adzhubei, A.; Spitz, L.; Lewis, P.; Goldfarb, D.; Emerman, M.; Stevenson, M. A nuclear-localization signal within HIV-1 matrix protein that governs infection of nondividing cells. *Nature* **1993**, *365*, 666–669.

(2) Miller, M. D.; Farnet, C. M.; Bushman, F. D. Human immunodeficiency virus type 1 preintegration complexes: studies of organization and composition. *J. Virol.* **1997**, *71*, 5382–5390.

(3) Farnet, C. M.; Bushman, F. D. HIV-1 cDNA integration: Requirement of HMG I(Y) protein for function of preintegration complexes in vitro. *Cell* **1997**, *88*, 483–492.

(4) Chen, H.; Engelman, A. The barrier-to-autointegration protein is a host factor for HIV type 1 integration. *Proc. Natl. Acad. Sci. U.S. A.* **1998**, *95*, 15270–15274.

(5) Gleenberg, I. O.; Herschhorn, A.; Hizi, A. Inhibition of the activities of reverse transcriptase and integrase of human immunodeficiency virus type-1 by peptides derived from the homologous viral protein R (Vpr). *J. Mol. Biol.* **2007**, *369*, 1230–1243.

(6) Gleenberg, I. O.; Avidan, O.; Goldgur, Y.; Herschhorn, A.; Hizi, A. Peptides derived from the reverse transcriptase of human immunodeficiency virus type 1 as novel inhibitors of the viral integrase. *J. Biol. Chem.* **2005**, *280*, 21987–21996.

(7) Hehl, E. A.; Joshi, P.; Kalpana, G. V.; Prasad, V. R. Interaction between human immunodeficiency virus type I reverse transcriptase and integrase proteins. *J. Virol.* **2004**, *78*, 5056–5067.

(8) Tasara, T.; Maga, G.; Hottiger, M. O.; Hubscher, U. HIV-1 reverse transcriptase and integrase enzymes physically interact and inhibit each other. *FEBS Lett.* **2001**, *507*, 39–44.

(9) Gleenberg, I. O.; Herschhorn, A.; Goldgur, Y.; Hizi, A. Inhibition of human immunodeficiency virus type-1 reverse transcriptase by a novel peptide derived from the viral integrase. *Arch. Biochem. Biophys.* **2007**, *458*, 202–212.

(10) Bischerour, J.; Tauc, P.; Leh, H.; De Rocquigny, H.; Roques, B.; Mouscadet, J. F. The (52−96) C-Terminal domain of Vpr stimulates HIV-1 IN-mediated homologous strand transfer of mini-viral DNA. *Nucleic Acids Res.* **2003**, *31*, 2694–2702.

(11) Hayouka, Z.; Rosenbluh, J.; Levin, A.; Loya, S.; Lebendiker, M.; Veprintsev, D.; Kotler, M.; Hizi, A.; Loyter, A.; Friedler, A. Inhibiting HIV-1 integrase by shifting its oligomerization equilibrium. *Proc. Natl. Acad. Sci. U.S.A.* **2007**, *104*, 8316–8312.

(12) Yan, H.; Mizutani, T. C.; Nomura, N.; Tanaka, T.; Kitamura, Y.; Miura, H.; Nishizawa, M.; Tatsumi, M.; Yamamoto, N.; Sugiura, W. A novel small molecular weight compound with a carbazole structure that demonstrates potent human immunodeficiency virus type-1 integrase inhibitory activity. *Antivir. Chem. Chemother.* **2005**, *16*, 363–373.

(13) Suzuki, T.; Futaki, S.; Niwa, M.; Tanaka, S.; Ueda, K.; Sugiura, Y. Possible existence of common internalization mechanisms among arginine-rich peptides. *J. Biol. Chem.* **2002**, *277*, 2437–2443.

(14) Wender, P. A.; Mitchell, D. J.; Pattabiraman, K.; Pelkey, E. T.; Steinman, L.; Rothbard, J. B. The design, synthesis, and evaluation of molecules that enable or enhance cellular uptake: Peptoid molecular transporters. *Proc. Natl. Acad. Sci. U.S.A.* **2000**, *97*, 13003–13008.

(15) Matsushita, M.; Tomizawa, K.; Moriwaki, A.; Li, S. T.; Terada, H.; Matsui, H. A high-efficiency protein transduction system demonstrating the role of PKA in long-lasting long-term potentiation. *J. Neurosci.* **2001**, *21*, 6000–6007.

(16) Takenobu, T.; Tomizawa, K.; Matsushita, M.; Li, S. T.; Moriwaki, A.; Lu, Y. F.; Matsui, H. Development of p53 protein transduction therapy using membrane-permeable peptides and the application to oral cancer cells. *Mol. Cancer Ther.* **2002**, *1*, 1043–1049.

(17) Wu, H. Y.; Tomizawa, K.; Matsushita, M.; Lu, Y. F.; Li, S. T.; Matsui, H. Poly-arginine-fused calpastatin peptide, a living cell membrane-permeable and specific inhibitor for calpain. *Neurosci. Res.* **2003**, *47*, 131–135.

(18) Rothbard, J. B.; Garlington, S.; Lin, Q.; Kirschberg, T.; Kreider, E.; McGrane, P. L.; Wender, P. A.; Khavari, P. A. Conjugation of arginine oligomers to cyclosporin A facilitates topical delivery and inhibition of inflammation. *Nature Med.* **2000**, *6*, 1253–1257.

(19) Marchand, C.; Zhang, X.; Pais, G. C. G.; Cowansage, K.; Neamati, N.; Burke, T. R., Jr.; Pommier, Y. Structural determinants for HIV-1 integrase inhibition by beta-diketo acids. *J. Biol. Chem.* **2002**, *277*, 12596–12603.

(20) Semenova, E. A.; Johnson, A. A.; Marchand, C.; Davis, D. A.; Tarchoan, R.; Pommier, Y. Preferential inhibition of the magnesium-dependent strand transfer reaction of HIV-1 integrase by alpha-hydroxytropolones. *Mol. Pharmacol.* **2006**, *69*, 1454–1460.

(21) Parniak, M. A.; Min, K. L.; Budihas, S. R.; Le Grice, S. F. J.; Beutler, J. A. A fluorescence-based high-throughput screening assay for inhibitors of HIV-1 reverse transcriptase associated ribonuclease H activity. *Anal. Biochem.* **2003**, *322*, 33–39.

(22) Morellet, N.; Bouaziz, S.; Petitjean, P.; Roques, B. P. NMR structure of the HIV-1 regulatory protein Vpr. *J. Mol. Biol.* **2003**, *327*, 215–227.

(23) Karki, R. G.; Tang, Y.; Burke, T. R., Jr.; Nicklaus, M. C. Model of full-length HIV-1 integrase complexed with viral DNA as template for anti-HIV drug design. *J. Comput.-Aided Mol. Des.* **2004**, *18*, 739–760.

(24) Wallace, A. C.; Laskowski, R. A.; Thormton, J. M. LIGPLOT—a program to generate schematic diagrams of protein ligand interactions. *Protein Eng.* **1995**, *8*, 127–134.

(25) Li, H.-Y.; Zawahir, Z.; Song, L.-D.; Long, Y.-Q.; Neamati, N. Sequence-based design and discovery of peptide inhibitors of HIV-1 integrase: insight into the binding mode of the enzyme. *J. Med. Chem.* **2006**, *49*, 4477–4486.

Journal: Gt | ☐ Disk used | Despatch Date: 6/4/2010
Article : npg_gt_gt201061 | Pages: 1–10 | OP: XXX ED: XXX CE: XXX Graphic: Fig 1 color

Gene Therapy (2010), 1–10

www.nature.com/gt

ORIGINAL ARTICLE

Improvement of lentiviral vector-mediated gene transduction by genetic engineering of the structural protein Pr55^{Gag}

T Aoki[1,2], S Shimizu[1], E Urano[1,3], Y Futahashi[1], M Hamatake[1], H Tamamura[2], K Terashima[4], T Murakami[1], N Yamamoto[1] and J Komano[1]

[1]AIDS Research Center, National Institute of Infectious Diseases, Tokyo, Japan; [2]Institute of Biomaterials and Bioengineering, Tokyo Medical and Dental University, Tokyo, Japan; [3]Kitasato Institute of Life Sciences, Kitasato University, Tokyo, Japan and [4]Department of Comprehensive Pathology, Aging and Developmental Sciences, Tokyo Medical and Dental University, Graduate School, Tokyo, Japan

The lentiviral vector is a promising tool for human gene therapy because of its ability to transduce genes into many cell types. However, one of the technical problems associated with the lentiviral vector is that lentiviral titers in current production systems are relatively low compared with the other viral vectors. In this study, we provide genetic evidence that the attachment of heterologous myristoylation (myr) signals on the amino-terminus of human immunodeficiency virus type 1 Pr55^{Gag} (Gag) can increase the viral yield up to 10-fold, leading to the enhancement of gene transduction in many cell lines. The myr signal Gag constructs behaved similarly to the wild-type Gag in targeting to detergent-resistant membrane compartments, Vps4-dependence for viral budding, and virion morphology. However, the myr signal Gag constructs showed improved oligomerization efficiency as measured by bioluminescence resonance energy transfer in living cells, contributing to increased viral production and efficient activation of the viral protease responsible for virion maturation. The genetically modified Gag represents the next generation lentiviral vector, and should contribute to the success of many lentiviral vector applications.
Gene Therapy (2010) **0**, 000–000. doi:10.1038/gt.2010.61

Keywords: *lentiviral vector; gag; myristoylation*

Introduction

The lentiviral vector is a powerful tool for transduction of genes into many cell types, especially non-dividing cells such as neurons, and is being used in clinical trials of human gene therapies and other applications.[1–8] The use of lentiviral vectors has been made possible because of advances in basic virology and because of a series of modifications that have increased the safety of the lentiviral vector. The commonly used third-generation lentiviral vector is a *Tat*-independent four-plasmid system composed of a gene transfer vector and three trans-vectors expressing Rev, Env and Gag-pol. The gene transfer vector is equipped with a self-inactivation LTR system (SIN). Viruses are often pseudotyped by vesicular stomatitis virus G (VSV-G). The human codon-optimized *gag-pol* expression vector is used to increase viral yield.[9]

The application of the lentiviral vector to human gene therapy was first approved for the treatment of human immunodeficiency virus (HIV) infections in the early 2000s.[1]. Since then, because of its potential advantages, the use of lentiviral vector has been expanding. A large amount of lentiviral particle must be produced for clinical trials. A technical improvement to increase the viral titer obtained from a production system would have a substantial effect on the cost of supporting a clinical human gene therapy trial using the lentiviral vector. The lentiviral vector titer in current production systems is generally in the order of 10^5–10^6 transducing units per ml. Although titer can be increased by centrifugation, the production yield is not as high as other viral vectors including the widely used adenoviral vectors. The HIV-1-based lentiviral vector has been engineered to reduce the risk of pathogenicity associated with HIV-1 [5,9], which resulted in a decrease of the viral titer.

Retroviral production and infectivity are regulated by the amino-terminal matrix domain (p17^{MA} or MA) of Pr55^{Gag} (Gag).[10–13] The myristoylation (myr) signal in the MA is critical for efficient viral production by aiding Gag trafficking to the plasma membrane (PM). In a previous study, we found that substitution of the HIV-1 Gag myr with the phospholipase C-δ1 pleckstrin homology (PH) domain increased the production of the third-generation lentiviral vector in which the *gag-pol* is human codon-optimized.[14] This prompted us to search for a PM-targeting signal that could enhance viral production to a greater extent than PH-Gag. Among the PM-targeting signals, we discovered that the myr signal motifs of

Correspondence: Dr J Komano, AIDS Research Center, National Institute of Infectious Diseases, 1-23-1 Toyama, Shinjuku, Tokyo, 162, Japan.
E-mail: ajkomano@nih.go.jp
Received 9 November 2009; revised 23 February 2010; accepted 7 March 2010